Particle Accelerators, 1995, Vol. 79, pp. 79–120
Reprints available directly from the publisher
Photocopying permitted by license only

POWER TESTS OF A STRING OF MAGNETS COMPRISING A FULL CELL OF THE SUPERCONDUCTING SUPER COLLIDER

W. BURGETT,[1] L. CROMER,[1] D. HAENNI,[1] M. HENTGES,[1] T. JAFFERY,[1] P. KRAUSHAAR,[1] M. LEVIN,[1] A. McINTURFF,[2] G. MULHOLLAND,[1] D. RICHTER,[1] W. ROBINSON,[1] D. VOY,[3] J. WEISEND II[1] and J. ZATOPEK[1]

[1]*Superconducting Super Collider Laboratory, 2275 Highway 77, North Waxahachie, TX 75135, USA*

[2]*Lawrence Berkeley Laboratory, 1 Cyclotron Road, Berkeley, CA 94720, USA*

[3]*Fermi National Accelerator Laboratory, Batavia, IL, USA*

(Received 6 February 1995; in final form 29 June 1995)

In this paper we describe the operation and testing of a string of magnets comprising a full cell of the Superconducting Super Collider (SSC). The full cell configuration composed of ten dipoles, two quadrupoles, and three spool pieces is the longest SSC magnet string ever tested. Although the tests of the full cell were undertaken after the SSC project was marked for termination, their completion was deemed necessary and useful to future efforts at other accelerator laboratories utilizing superconducting magnets. The focus of this work is on the electrical and cryogenic performance of the string components and the quench protection system with an emphasis on solving some of the questions concerning electrical performance raised during the previous two experimental runs involving a half cell configuration.

KEY WORDS: Magnetic measurements, magnets: superconducting

1 INTRODUCTION

The Accelerator Systems String Test (ASST) facilities of the Superconducting Super Collider Laboratory (SSCL) were located at the N15 site in Ellis County near Waxahachie, Texas. This complex was constructed in 1991 to demonstrate the operation of a standard half cell of the collider machine using prototypical industrially-produced magnets. The successful operation on August 14, 1992 at a current of 6520 amperes, 20 amperes above the collider's designed operating current, marked the completion of a Congressionally-mandated M1 milestone six weeks ahead of schedule, Run #1.[1–3] The ASST half cell consisted of five 50-mm aperture dipoles, one 40-mm aperture quadrupole, and three spool

pieces. The dipoles were assembled at Fermi National Accelerator Laboratory (FNAL) by technicians from General Dynamics using the laboratory-developed design and tooling. The spool pieces were manufactured by industrial sub-contractors using an SSCL design, and the quadrupole coldmass was built at Lawrence Berkeley Laboratory (LBL) and placed in its cryostat at the SSCL. Prior to installation at the ASST, the dipole magnets were cold-tested in single magnet tests at FNAL and the quadrupole coldmasses at LBL.

The completion of the milestone marked a transition point for the ASST in that the management structure and milestone task force were restructured in order to use the facility as an ongoing research and development test bed for collider lattice components. The underlying philosophy was that the SSCL required a facility where technical components could be integrated into collider prototypical systems and subsystems for testing under various operational scenarios. In addition to testing components and systems response, the ASST allowed critical training of operations and safety personnel.[4]

Subsequent to the completion of the M1 milestone, a series of power tests and experiments were conducted on the original half cell configuration from November 1992 through January 1993, Run #2.[5–8] During that time, and during some of the tests conducted prior to the achievement of the milestone, it was noticed that the magnet string developed higher than expected voltages-to-ground. It also appeared that at the higher currents, quench propagation was occurring from one quarter cell to the next due to thermal conduction from the helium heated by the original quench (each half cell is divided into two quarter cells for quench protection purposes; see Reference 3 and Section 2 for details). Thus, in order to address these issues, and to conduct other experiments crucial to characterizing magnet behavior and quench protection system performance in a full cell configuration, a proposal was made to the Department of Energy (DOE) to allow a final full cell run before ASST decommissioning. The DOE approved sufficient funds for a six week power testing period undertaken in January and February 1994. Although this was a relatively short amount of time, more than 50 quench events were initiated, experiments aimed at addressing seven separate issues were carried out, and enough data was collected to definitively answer the majority of questions raised prior to testing. Moreover, the data also clearly indicates new areas needing investigation and clarification in future similar tests at other facilities.

For the tests involving a full cell, the string components consisted of the five dipole magnets, feed spool, and end spool from the original half cell plus two other FNAL dipoles, three dipole magnets constructed at the Brookhaven National Laboratory (BNL), two new LBL quadrupoles, and a new mid-cell spool (SPR ≡ spool piece with recooler). As discussed in Reference 2, the electrical behavior of the magnets in a half cell configuration was different from that observed during single magnet testing (e.g., the higher than expected voltages-to-ground). Similarly, the performance of the quench protection system showed important differences during the full cell tests from that observed during the half cell tests.[7] Since the quench protection system envisioned for the superconducting magnets to be used in the Large Hadron Collider (LHC) at CERN has similar functionality as the SSC design (except the voltage is divided by a cold diode for either each dipole or dipole aperture),[9–11] the results described in this paper should provide useful insights applicable to the upcoming LHC string tests.

The thermal heat leak measurements collected during the Fall of 1993 are presented which were intended to answer, but did not provide definitive resolution to, the question of

whether the cryostats of the magnets and spools provided adequate insulation and isolation for meeting budgeted design refrigeration loads. However, the quantity and quality of the data that was collected can provide useful inputs to future efforts to model and simulate magnet cryostat thermal performance.

2 STRING COMPONENT CHARACTERISTICS AND STRING CONFIGURATION

After the conclusion of the half cell tests (January 1993), the extension and reconfiguration of the string into a full cell was initiated. Based on the preliminary results from these tests, the principal consideration given in the reconfiguration design was to group magnets with similar outer coil low temperature normal state resistance (RRR) into quarter cells corresponding to the quench protection system's (QPS) protection units composed either of three dipoles or two dipoles and a quadrupole. The Residual Resistivity Ratio (RRR) is the ratio of resistivity at 300 K to a low temperature resistivity, usually measured around 10 K. The RRR values were matched to approximately 10% within a protection unit across the full cell. This grouping was motivated by higher than expected voltages observed during quenching in the half cell tests where the RRR values of the outer coils varied by approximately a factor of two within a quarter cell. The original half cell had DCA313, DCA314 and DCA319 in the first quarter cell, followed by DCA315, DCA316 and QCC403 in the second. By matching the RRR, it was hoped that these voltages would be reduced (see Section 4.1). Table 1 contains the RRR values for the dipole outer coils used in the full cell grouped by quench protection units.[12–16] The "SS" values were obtained from short sample testing prior to coil fabrication. The "Test" values were measured on the completed

TABLE 1: Measured RRR values for the full cell magnets.

	Upper outer coil		Lower outer coil	
	SS	Test	SS	Test
DCA313	39	174	38	171
DCA314	41	177	38	174
DCA315	41	173	41	174
DCA323	39	102	39	121
DCA322	40	113	40	112
DCA316	39	109	39	109
DCA319	42	96	42	97
DCA320	39	98	39	99
DCA210	41	217	41	209
DCA212	37	231	37	227
QCC405	na	119		
QCC406	na	104		

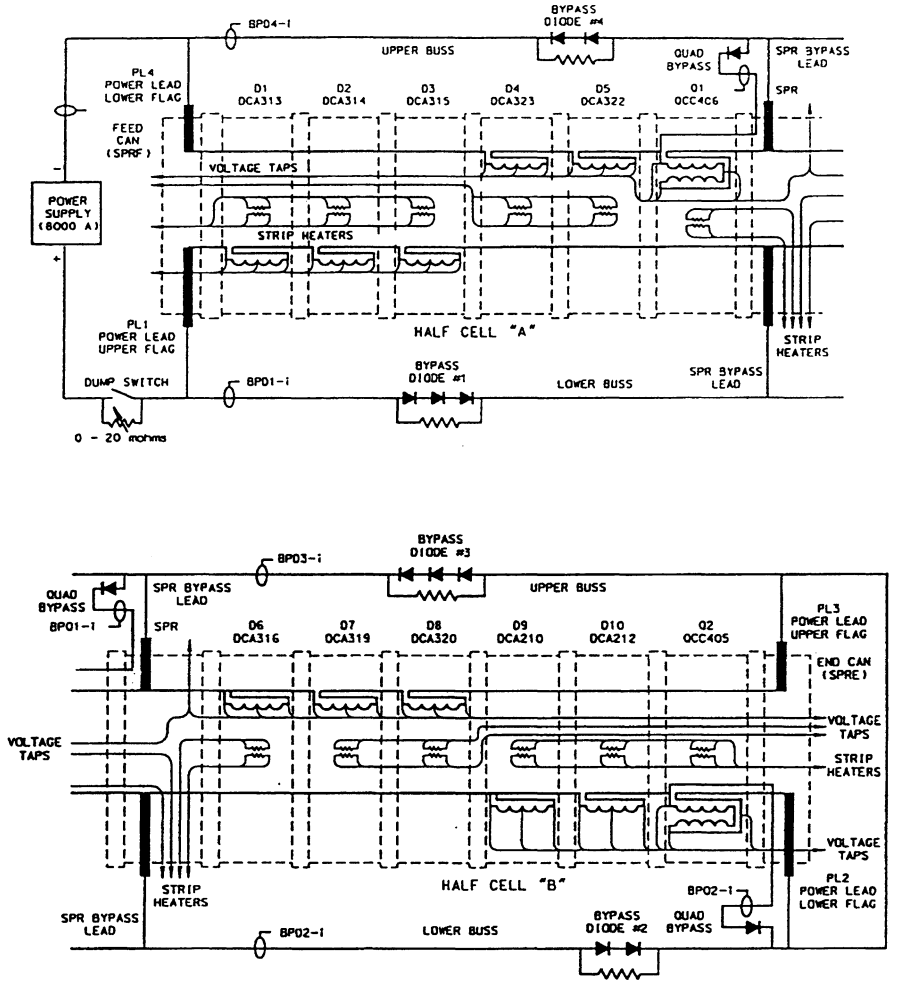

FIGURE 1: This graphical representation of the full cell circuit shows the high current main circuits (upper and lower busses). It also shows the quench detection voltage taps, protection strip heater circuits, the quench bypass circuits, the current monitoring points and the voltage limiting diodes. It is important to remember that the bypasses and diodes are room temperature transient circuits. This is also true of the power supply and dump switch.

magnets during single magnet testing. The wide variation between the SS values and the ones for the fabricated coils is presumed to result from differences in the coil curing process. The FNAL fabricated coils for DCA311 through DCA319 used the standard kapton/glass insulation and were cured at approximately 135°C. DCA320 and DCA321 had all kapton insulated coils cured at 170°C. DCA322 and DCA323 used an apical insulation with a cryorad adhesive and were cured at 170°C. The DCA200's series magnets were fabricated at BNL. DCA207 through DCA211 used the standard kapton/glass insulation and the

standard cure at about 135°C. DCA212 and DCA213 used an all kapton insulation with a polyimide adhesive and a modified cure at 225°C.[17] Cure times were on the order of a few hours.

A generalized electrical schematic of the ASST full cell showing the order and placement of the magnet string components and the principal elements of the power and quench protection systems is shown in Figure 1. Due to the various integrated energy density capacities of the cables used to fabricate the magnet coils (20, 16, and 10×10^6 A^2–s for the dipole inner, outer and quadrupole coil cables, respectively), the quadrupoles required an individual bypass lead and diode configuration. The bypass diode stacks were passive devices that would not conduct with the voltages developed during ramping (at 4 A/s) under normal conditions but would with the large positive voltages possible during a quench. Current transductors measured the current in each bypass circuit along with the total current from the power supply, and the current in each magnet was then calculated from the measured quantities. The dump switch was in series with the power supply, and consisted of a mechanical high current switch in series with SCRs. The SCRs were the primary switch with a mechanical switch as backup. One short test was conducted where the mechanical switch was used without the SCRs, and it functioned properly. However, during Run 3 a number of ramp aborts occurred due to the mechanical switch failing (going open) which was a cause of concern for the reliability of the switch's design. During ASST testing this was an inconvenience, but during actual accelerator operations this would present a more serious down time problem.

The QPS for the full cell monitored voltage-to-ground points around the full cell circuit along with half coil voltage taps from each magnet. Resistive voltages for the magnet coils and all sections of superconducting buss were calculated from these measured values. The resistive voltages were used for the purpose of determining the existence of a quench condition. However, the algorithm used by the quench protection monitor (QPM) to calculate the resistive voltages became unreliable once the quench protection function of the QPM was activated. For this reason, the resistive voltages for the analysis were reconstructed independently from the actual measured voltages as part of the off line data analysis effort. For some magnets, quarter coil voltages were recorded as part of the R&D instrumentation system (RIDAS), but were not used by the QPS for quench detection. In order to test the QPS architecture, two individual quench protection monitors were used, one for half cell A and one for half cell B. The two QPMs operated independently and communicated through the QPS to the power supplies and the operator consoles. Each QPM contained circular data buffers capable of storing twenty seconds of data. In the event of a quench in a magnet protected by one QPM, that QPM fired the protection heaters and recorded the quench data in its circular buffers while the remaining QPM continued to monitor its magnets for any possible quenches. Initially, the time zero for the data collected by each QPM was the time of the event detected which caused the QPM to activate its protection function. Later, in order to find the proper time sequencing of events which occurred in each half cell during a single quench test, the two data buffers from QPM1 and QPM2 were referenced to a common time base which used the time of the initial event as time zero. This was necessary for the data analysis effort.

Reference 7 contains a discussion of the pre-operations testing and the process used to commission the full cell magnet string.

3 STRING CRYOGENIC OPERATION

One important operational difference for the full cell string test (Run 3) from the previous two half cell string tests (Runs 1 and 2) was the use of a new refrigerator and cryogenics system.[7] Because the cryogenics system (denoted Plan A) initially intended for the ASST was not ready in time to support the milestone string test, a smaller 550 watt helium refrigerator (Plan B) had to be used.[3,6] This backup system could provide up to 135 l/hr of liquid helium, could deliver a 50 g/s helium mass flow, and was adequate for cooling and operating the half cell string. The Plan B refrigerator was removed from the ASST after the completion of Run 2, and would have been used to provide liquid helium to the spool piece test stand at the SSCL's Central Facility.

The Plan A refrigerator was commissioned in August 1993, and was used for cooling and operating the full cell string during the thermal heat leak tests in the Fall of 1993[6] as well as during the Run 3 power tests. The Plan A refrigerator was one of three coldboxes (with similar capacities) that were installed at the N15 site. One of the coldboxes was installed in the SSCL Magnet Test Laboratory (MTL) to support test stand operations. The third coldbox was installed in the N15 Arc Sector Refrigerator building (with the Plan A one) and would have been part of that sector refrigerator for the collider machine. The Plan A system was tested at 4500 watts of refrigeration at 0 g/s of liquefaction, and, during normal operations, could provide 2200 watts of refrigeration with 22 g/s of liquefaction (out of a maximum of 40 g/s). The nominal mass flow for the Run 3 power tests was 100 g/s. The minimum flow capability was 20 g/s, and the designed minimum operating temperature was 3.8 K. The temperature was kept between 3.8 K and 4.5 K for the string test at an operating pressure of 4 bar. A block diagram of the Plan A system is shown in Figure 2 with the connections and flow relationships to the ASST shown in Figure 3.

It is worthwhile noting the significant increase in operational capability of the Plan A system that occurred during the Run 3 power tests. At the beginning of the high power testing (above 6000 amperes), a quench resulted in taking the refrigerator off-line due to the quench pressure relief and heating causing compressor stalls. However, after some changes in software and greater operator experience, these problems were overcome, and a quench subsequently had a minimal effect on refrigerator operations enabling one to two hour operational recovery times.

4 FULL CELL COMMISSIONING AND QUENCH TESTING

Before describing the details of the quench tests, it is important to mention that during the process of operational certification of the magnet string a high pressure leak from the cold helium piping to the insulation vacuum in the SPR was discovered. This leak was similar to one previously found in a different SPR that was used in the half cell tests,[5] and appeared to originate from the same area near the recooler valves. The system would certify to 10^{-9} cm^3/s of standard He up to a threshold pressure, then suddenly degrade to 10^{-8} cm^3/s, and continue to degrade further with increasing pressure until reaching a leak rate of order 10^{-7} cm^3/s at 1.85 MPa (the highest pressure used for certification). The SPR used in the half cell tests had a threshold pressure of approximately 1 MPa while

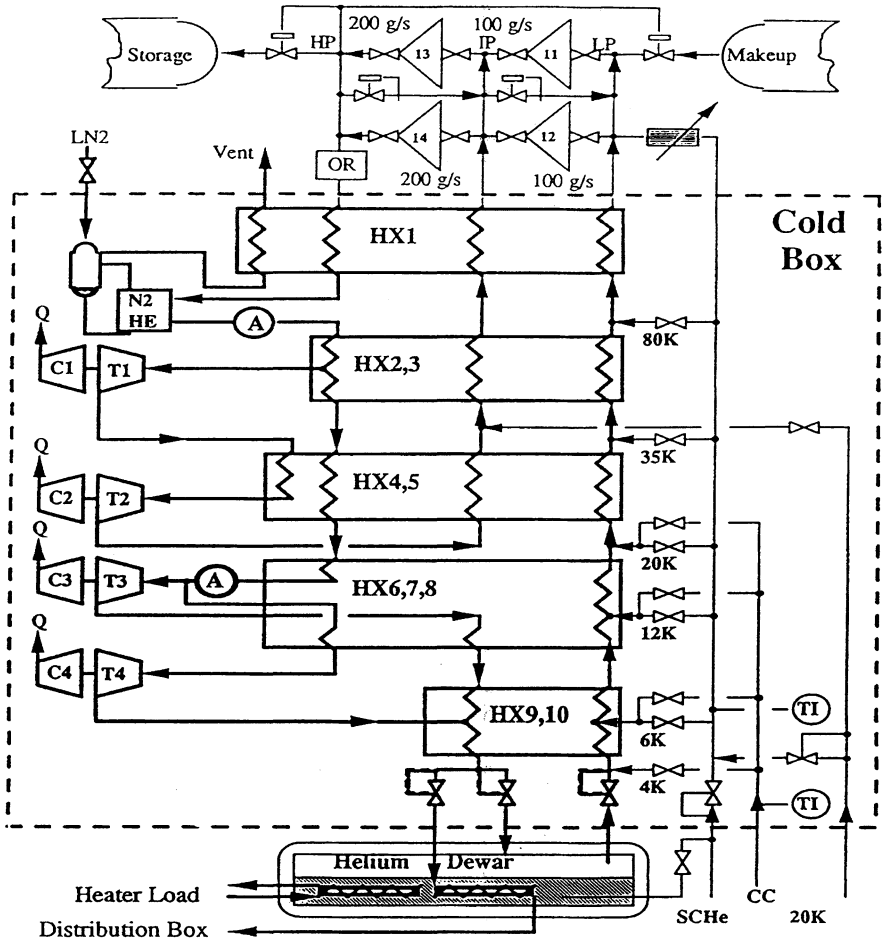

FIGURE 2.: This is the flow diagram of the plan "A" refrigerator which was used for the full cell tests. It was a nominal 4.5 kilowatt, 4.35 K, 100 gram/second helium refrigerator.

the threshold pressure of the SPR used in the full cell tests was about 1.44 MPa which is very close to the cracking pressure of the safety valves. The unique features of these leaks were that (i) the threshold pressure was independent of temperature, and (ii) the leaks were not detectable below the threshold even after recycling the pressure several times. As a precautionary measure, additional vacuum pumps were used, but the presence of the leak did not affect operations. Since the leak characteristics were very similar in two different spools, it is hypothesized that this problem is due to a design flaw in the SPR cold helium piping and valving, but this has not been verified.

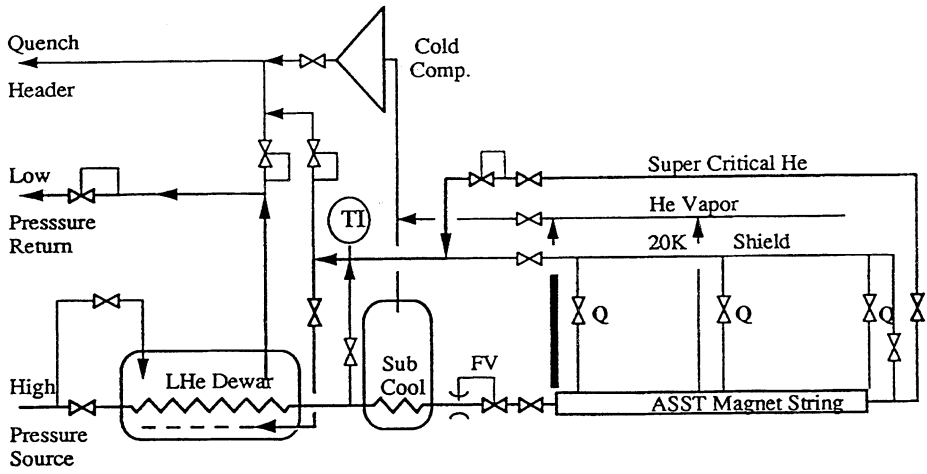

FIGURE 3: The cryogenic flow diagram for the full cell as used during the late 1993 and early 1994 test period.

The power testing of the full cell string began on January 14, 1994 with a series of 2000 ampere strip heater induced quenches. The time delays (Δt) from heater firing to the first detectable resistance (R_i) and one resistive volt (V_R) are shown in Table 2. The data for these quenches show that the response of all the dipoles is very similar. The purpose of these low current quenches was to ensure that the strip heater circuits and the QPS logic were functioning according to design. After the initial checks at 2000 amperes, strip heater induced quenches were initiated at increasing increments of current until the full field level of 6600 amperes was reached on February 3, 1994. Two spontaneous quenches occurred before reaching the full field level, one in dipole 6 and one in dipole 10, but both occurred above 5900 amperes (a detailed discussion is given later).

The DCA 323 and DCA 322 heater study data shown in Table 3 for D5 (DCA322) give a typical set of numbers for strip heater initiated quenches as a function of magnet current. These data show a factor of 5 to 10 gain in heater effectiveness from a current slightly over the cryo-stable point (2000 amperes) to the peak operating current (6500 amperes). The energy requirements for both standard and experimental heaters are less in these two magnets because only half the amount of Kapton insulation (one 5 mil layer instead of two layers) was used between the heater strips and the magnet coils.[18]

The experimental plan for the full cell run included tests aimed at addressing the following issues:

1. Could the high voltages-to-ground observed in Runs 1 and 2 be significantly reduced by matching dipole outer coil RRR values within a quarter cell protection unit?

2. Could the quench be contained within the quarter cell protection unit where it originated?

3. Was there sufficient critical current margin to operate the string up to 7000 amperes (~7 T)?

TABLE 2: 2000 AMP heater commissioning results.

Magnet	Heater Type	$t(\text{HF}\rightarrow R_i)$(s)	$t(\text{HF}\rightarrow 1V_R)$(s)
D1-DCA313	Standard (HE)	0.168	0.200
D2-DCA314	Standard (HE)	0.168	0.200
D3-DCA315	Standard (HE)	0.184	0.236
D4-DCA323*	Exp. Type 1 (LE)	0.250	0.620
D4-DCA323*	Standard (HE)	0.116	0.167
D5-DCA322*	Exp. Type 2 (LE)	0.116	0.200
D5-DCA322*	Standard (HE)	0.116	0.162
D6-DCA316	Standard (HE)	0.133	0.175
D7-DCA319	Standard (HE)	0.133	0.175
D8-DCA320	Standard (HE)	0.150	0.200
D9-DCA210	Standard (HE)	0.135	0.170
D10-DCA212	Standard (HE)	0.125	0.187

*The amount of Kapton insulation between the strip heater and the magnet coil was reduced to 25 microns from the standard 50 microns thickness in these magnets. This was done by reducing the number of Kapton layers (or wraps) from two to one, eliminating a possible He boundary.

TABLE 3: Heater study results from magnet D5 (DCA322).

Current	Heater Type	$t(\text{HF}\rightarrow R_i)$ seconds	$t(\text{HF}\rightarrow 1V_R)$ seconds	τ(decay) seconds	MITS
2000	LE	0.15	0.233	1.674	4.01
2000	Standard	0.046	0.162	0.881	2.03
3000	LE	0.10	0.125	1.053	4.96
5000	LE	0.02	0.055	0.48	6.75
5500	LE	0.035	0.053	0.40	5.86
6000	LE (@ 4.5 K)	0.020	0.037	0.36	7.2
6000	LE (@ 3.9 K)	0.017	0.050	>0.375	8.55
6500	LE	0.020	0.037	>0.333	7.5

4. How would the string behave electrically at full field during spot heater induced quenches (which simulate spontaneous quenches)?
5. Could the quarter cell quench protection unit be enlarged to a half cell protection unit without risk to the string components?
6. Could the newly designed "low-energy" strip heaters protect the magnets as well as the older "high-energy" heaters?[18]
7. Would a catastrophic insulating vacuum breakdown to air adversely affect the string's cryogenic integrity or impact personnel safety?

In the course of these studies, data were also collected and analyzed concerning pressure wave propagation, the two spontaneous quenches, and as an unanticipated part of addressing issue #2 above, a great deal of information was obtained regarding the ramp-rate dependence of AC loss induced heating and quenching. A few weaknesses in the QPS logic and hardware design were also exposed and characterized in the course of performing the above experiments.

4.1 Electrical characteristics of RRR matched quarter cells

After higher than expected voltages-to-ground were observed in strip heater induced quench testing conducted during Runs 1 and 2, it was hypothesized that their presence was due to large differences in dipole outer coil RRR values within a quarter cell.[12] Thus, the ten dipoles used for the full cell tests were sorted according to their outer coil RRR values and separated into low and high RRR groups. The dipoles with relatively high values were placed on the lower power buss, and those with relatively low values were placed on the upper power buss. The magnets were additionally sorted to get as similar as possible RRR values within each quarter cell (see Table 1).[12–14,16] For strip heater induced quenches, the relevant coils are the outer coils, whereas for inner coil spontaneous quenches the inner coil RRR values become important (or for spot heater quenches if the spot heater is located on an inner coil).

As an example showing that the dipoles were indeed sorted by RRR, the resistance growth is shown in Figure 4 for 4000 A strip heater induced quenches initiated at the same operating temperature for D2, D6, and D7. The low RRR magnets, D6 and D7, should have higher low temperature resistances than the high RRR magnet, D2, since their room temperature resistances were measured to be equal. The data in Figure 4 clearly shows the expected similarity of D6 and D7 as well as the expected differentiation of D6 and D7 from D2.

It is also interesting to note the difference in the MIITS values for strip heater induced quenches for the high and low RRR groups as shown in Figure 5. Recall that the definition of the MIITS arises from a re-arrangement and integration of the heat balance equation of an adiabatic approximation for a one-dimensional conductor,

$$\int_0^t I^2(t)dt = A^2\rho \int_{T_0}^{T_f} \frac{C(T)}{R(T, B)} dT$$

where $I(t)$ is the current, $R(T, B)$ is the electrical copper resistivity, ρ is the density, A is the cross-sectional area, $C(T)$ is the specific heat and B is the magnetic field. MIITS is then defined as the value of the left hand side of the equation multiplied by 10^{-6}. Using the numerical approximation to the integral on the right-hand side, it is possible to solve for the adiabatic (maximum possible) temperature T_f of the conductor for a given value of MIITS. Since the high RRR magnets have more resistance to develop compared to the low RRR group, it takes a slightly longer time for the current to decay resulting in slightly higher MIITS values. This is shown in Figure 6 for two 6500 ampere quenches. Since the MIITS value indicates the temperature rise in the coil, it can be seen that those magnets

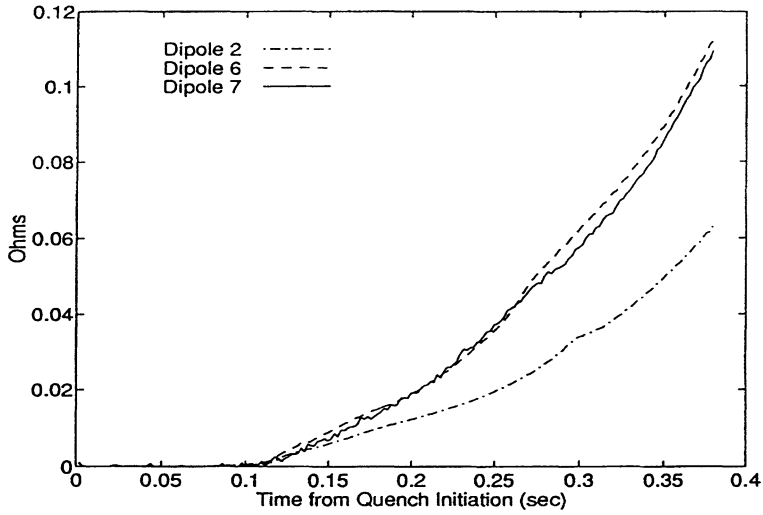

FIGURE 4: The resistance of three magnets (dipoles) in the full cell as a function of time after a quench initiated by a strip heater clearly shows the different response of the low temperature high resistance (low RRR) magnets to the low resistance (high RRR) ones.

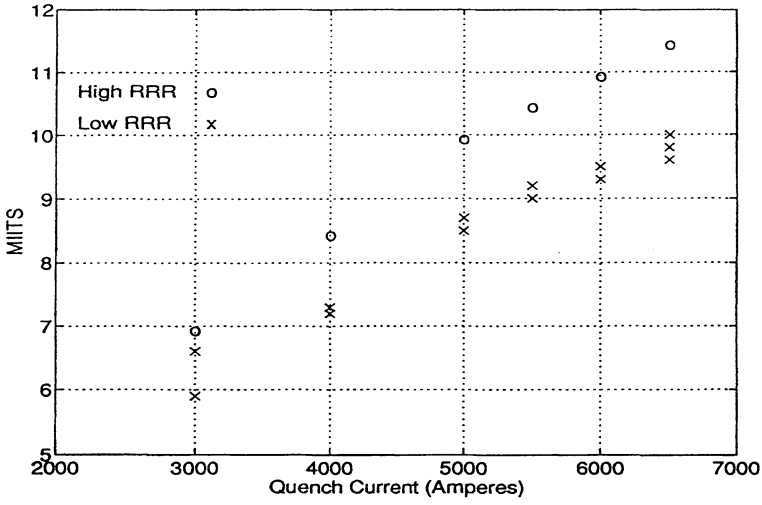

FIGURE 5: This plot of MIITS for quench events initiated by the protection strip heaters as a function of magnet current shows two clear groupings of magnets according to their low temperature resistance (RRR).

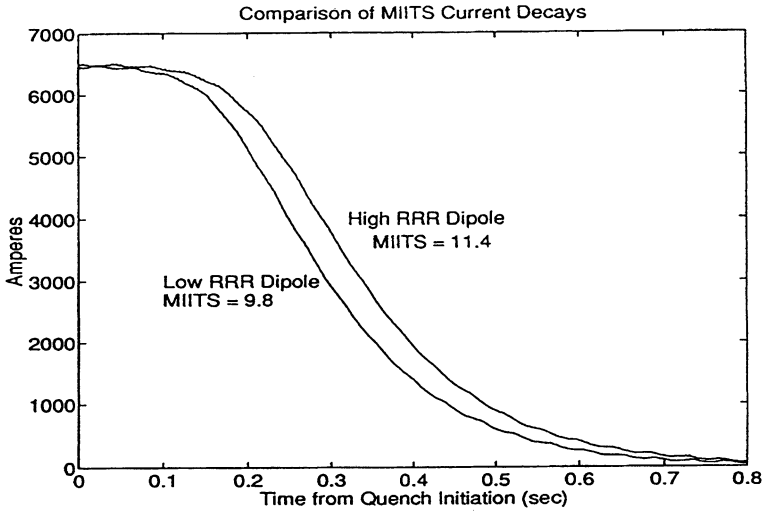

FIGURE 6: The plot of current in the magnet as a function of time shows the effect of low temperature resistance on the current decay of the protection unit, one with high resistance (low RRR) and one with low resistance (high RRR).

with high RRR values will develop higher coil temperatures at a given current compared to the low RRR magnets.

Table 4 presents measured voltages and calculated MIITS values for both high and low RRR magnets for strip heater induced quenches. The values in this table indicate the following trends for matched RRR quarter cells:

1. MIITS is a single magnet property dependent on RRR,
2. Voltage-to-ground depends on
   (i) location of quarter cell containing the quenching magnet within half cell (front, 3 dipoles; back, 2 dipoles plus quadrupole),
   (ii) position of quenching magnet within its quarter cell,
3. Max./Min. Coil Voltage (measured between input and output leads) depends mostly on whether the quenching magnet is in a front or back quarter cell. Front side is defined as that closest to the feed spool (SPRF) (see Figure 1).

Figures 7(a) and 7(b) give the voltage-to-ground traces for two different 6600 A quenches and shows the expected electrical similarity of quenches initiated at the same magnet positions in two different half cells.

The results of grouping the magnets according to their RRR values are conclusive in demonstrating that the voltages-to-ground are substantially reduced compared to having magnets with greatly differing RRR values in the same quarter cell as occurred in the

TABLE 4: MIITS and voltage to ground data for strip heater quenches.

Magnet	I_{max}	MIITS	VTG_{max}	VTG_{min}	Coil V_{max}	Coil V_{min}
			Lower Buss "A" Strip Heater Quenches (High RRR)			
D2	3000	6.9	37	–84	95	–49
D2	4000	8.4	149	–172	318	–162
D3	5000	9.9	631	–101	669	–335
D2	5500	10.4	508	–493	988	–523
D3	6000	10.9	1274	–118	1317	–657
D3	6500	11.4	1662	–126	1580	–854
			Upper Buss "B" Strip Heater Quenches (Low RRR)			
D6	3000	5.9	129	–29	146	–85
D6	4000	7.2	397	–24	415	–234
D7	4000	7.3	240	–151	375	–245
D7	5000	8.5	451	–289	724	–454
D7	5500	9.0	573	–365	880	–576
D7	6000	9.3	727	–543	1273	–730
D6	6500	9.6	1615	–93	1650	–958
D6	6500	9.8	1714	–47	1671	–995
			Upper Buss "A" Strip Heater Quenches (Low RRR)			
D5	3000	6.6	41	–51	98	–76
D5	5000	8.7	78	–271	251	–455
D5	5500	9.2	86	–453	473	–470
D5	6000	9.5	113	–532	623	–560
D5	6500	10.0	163	–648	770	–679

previous half cell runs (see Figure 8). The voltage-to-ground values plotted in Figure 8 are values from strip heater induced quenches of both high and low RRR dipoles. The maximum observed voltage-to-ground (VTG) in the half cell runs has a cubic dependence with an empirical least-squares approximation fit giving a correlation coefficient greater than 0.999, thus allowing a confident extrapolation to 6500 amperes; for safety reasons, no strip heater quench was initiated at 6500 amperes in the magnet generating the highest voltages predicted during the half cell runs. The 400–450 volt reduction in the maximum measured voltages-to-ground for the 6500 ampere strip heater induced quenches in the full cell tests compared to the extrapolated value for the half cell data is enough to eliminate any danger of an electrical breakdown of the magnets or spools. Note that, due to an electronics problem, the quench detection threshold for the matched RRR events was 1.0 V, whereas it was 0.5 V for the unmatched RRR events. Although the difference in the time for developing resistive voltage from 0 to 0.5 V and 0 to 1.0 V is on the order of 2–15 ms, and the time scale to develop the maximum VTG is of the order of 300–500 ms, there is some evidence from circuit simulations that the maximum VTG value is sensitive to the quench detection

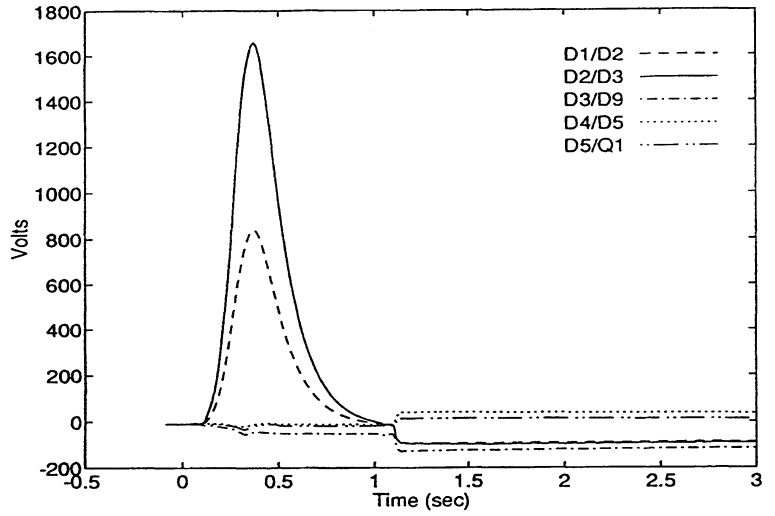

(a)

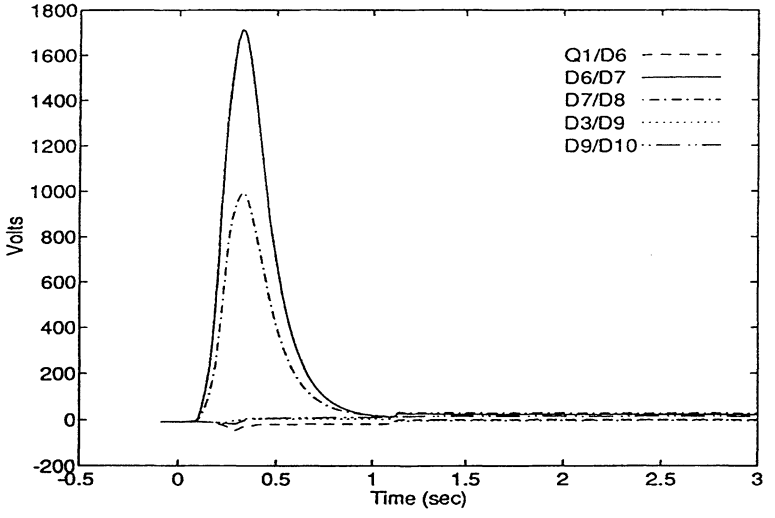

(b)

FIGURE 7: The voltages-to-ground between magnets are shown in plot 7(a) as a function of time is essentially the same as the plot in 7(b) even though the position of the low RRR magnets compared to the high RRR magnets is reversed. The current at the start of the strip heater induced quench in each case was 6500 amperes.

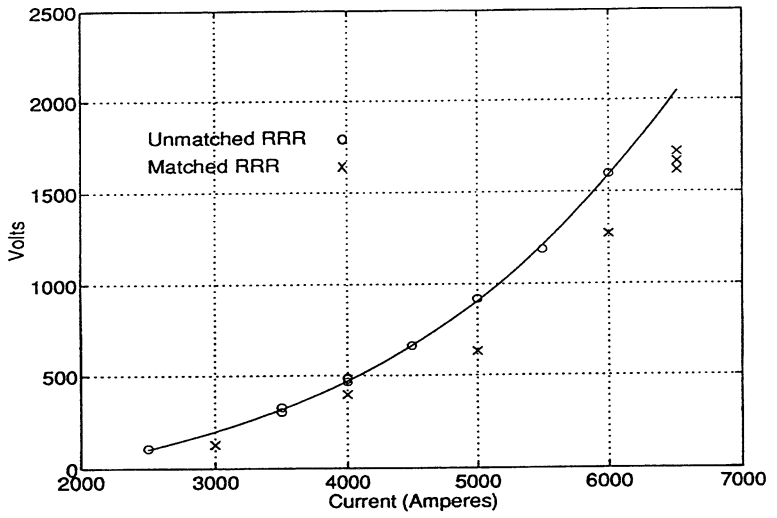

FIGURE 8: This plot of the peak voltage-to-ground between individual magnets as a function of the magnet current at a temperature of 4.5 K shows the difference in matching the RRR of the magnets in each protection unit (quarter cell in this case).

threshold.[15] Thus, the voltage-to-ground reduction from matching the RRR values of the dipoles may have been greater than presented here if a consistent threshold of 0.5 V had been used.

4.2 Quarter cell quench containment

As discussed previously, the quench protection system (QPS) is designed to protect the magnets in the event of a quench by firing protection strip heaters in the quenching quarter cell, bypassing the ring current around this quarter cell, and allowing current to be conducted through the magnets of the other quarter cells that remain superconducting during the time necessary for the string current to decay through an external dump resistor. Thus, the capability to contain a quench within a quarter cell is a major factor in determining the effectiveness of the QPS design. In the first two experimental runs involving only a half cell, quench propagation occurred from the first quarter cell to the first magnet of the second at currents above 4500 A, and was thought to be due to heat conducted through the helium from the originating quench. This view was reinforced by the observation that the quenches originated in the D4 upper inner coil as might be expected for a "thermally propagated" quench. However, the data collected during Run 3 indicate that quench propagation was occurring because of a strong ramp rate dependence of the dipole inner coils, and not due to the heat propagated through helium. Data showing the relative sensitivities of the dipoles to inner coil quenches from ramp rate induced heating had been previously obtained in single magnet tests.[14–16,19]

The ramping of a current through a superconducting magnet results in AC and magnetization losses in the cable that are manifested as heat. The losses result from eddy currents generated in the conductor by the changing magnetic field (due to the non zero dI/dt), from the hysteretic loss in the filaments, and both intrastrand and interstrand eddy currents. The magnitude of the interstrand eddy currents is directly related to the value of the cable's interstrand resistance, with lower values resulting in higher currents. Over a period of time, depending on the ramp rate magnitude, accumulated eddy current heating can generate a quench. The magnitudes of the up ramp rates at which this occurs are significantly less than the down ramp rate values because of the continual decrease in margin along the critical surface during up ramps. In the course of single magnet testing, a great deal of data was collected concerning dipole sensitivity to increasing current ramp rates because of the design requirement for Collider operation of 4 A/s. However, no data was collected in these tests concerning down ramp rate sensitivity, but the magnets most sensitive to up ramp rates should also be the most sensitive to down ramp rates. This appears to be a valid assumption given the quench behavior of the magnets observed during ASST Runs 1, 2, and 3.[1–3,5,7,20]

Secondary quenches in the ASST string occurred when the current down ramp rate magnitude exceeded a critical value. This resulted when a significant percentage of the inductance was removed from the power circuit, thus decreasing the L/R time constant, for example, when a quenching quarter cell was bypassed. The natural L/R time constant of the superconducting full cell (the inductance of all magnets divided by the resistance of the dump resistor) produced a decay current rate slower than the critical value. This condition was demonstrated repeatedly, albeit unintentionally, by frequent mechanical switch failures leading to successful current dumps at high string currents prior to the initiation of planned high current quenches.

The phenomenon of ramp rate induced secondary quenches became apparent during a string commissioning strip heater induced quench in D6. Dipole 6 quenched as expected, but D3 also quenched during the down ramp. The quarter cell containing D3 was separated from the quarter cell containing D6 by a quarter cell of non quenching magnets (D4, D5, Q1). Being cryogenically upstream from the D4-D5-Q1 quarter cell, however, the D1-D2-D3 quarter cell was colder. The magnets in the D1-D2-D3 quarter had all been found to exhibit significantly greater sensitivity to up ramp rates compared to D4 and D5 during single magnet testing with D3 (DCA 315) being the most sensitive.[16,18] In the previous half cell tests, DCA315 had been located in the D4 position.

An example of secondary quenches occurring because of ramp rate induced heating will now be discussed in detail. In this event, a 6500 A strip heater quench was initiated in D6. The secondary quench occurred in D3 at ~5.2 seconds later, and another ramp rate induced quench occurred in D10 at ~6.2 seconds. Because of the method used by the QPS software to calculate dI/dt in order to subtract the inductive contribution for the total voltage,[21] when the first and third quarter cells had quenched, the QPS detected a "relative dI/dt failure". Too few elements remained superconducting for the QPS to accurately calculate "dI/dt"; therefore causing it to activate the protection heaters in the second quarter cell (D4, D5, and Q1), resulting in the second quarter cell quenching at ~5.5 seconds. At least 50% of the elements need to be superconducting in order to accurately calculate "dI/dt". The quarter coil resistive voltages for D6, D3, and D10 are shown in Figure 9. From this figure it can be seen that the heat from the strip heaters caused the outer coils of D6 to quench first,

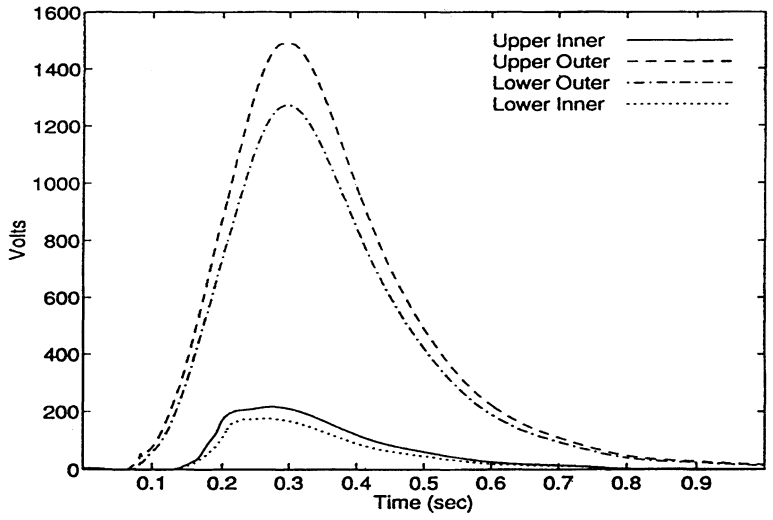
Upper Inner
Upper Outer
Lower Outer
Lower Inner
Volts
Time (sec)
1600
1400
1200
1000
800
600
400
200
0
0.1
0.2
0.3
0.4
0.5
0.6
0.7
0.8
0.9

(a)

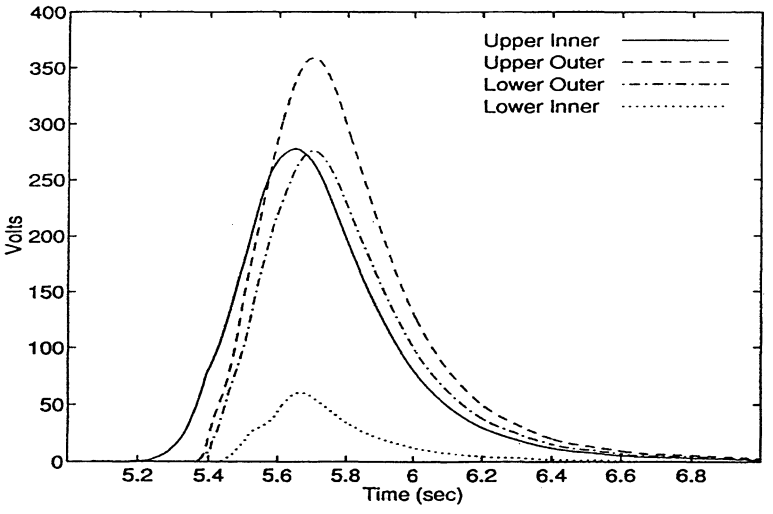
Upper Inner
Upper Outer
Lower Outer
Lower Inner
Volts
Time (sec)
400
350
300
250
200
150
100
50
0
5.2
5.4
5.6
5.8
6
6.2
6.4
6.6
6.8

(b)

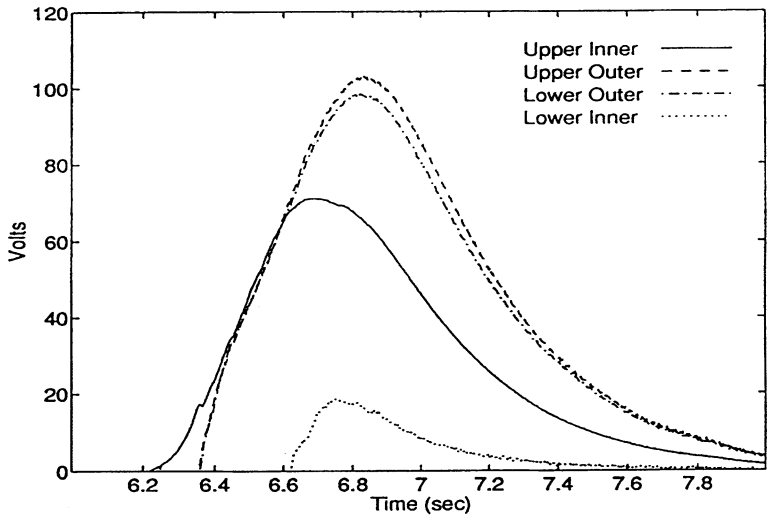

(c)

FIGURE 9: Resistive voltages for the magnets D6, D3, and D10 are plotted for a quench where the down ramp exceeds the critical rates for D3 and D10. The D6 outer coils are driven normal by the strip heaters, approximately 5.2 seconds later resistance appears in D3's upper inner winding due to an excessive down ramp, and then about one second later D10's upper inner winding appears resistive after the down ramp doubles due to the quenching of the quarter cell containing D3.

while the upper inner coils of D3 and D10 were the first quenching coils in these magnets as expected for a ramp rate induced quench. A plot of the magnet in each quarter cell that experienced the greatest resistive voltage is shown in Figure 10, and indicates the time evolution of the quenches throughout this event. As the current decayed, later quenching magnets developed smaller resistive voltages as expected, but not smaller MIITS values. The MIITS values for D6, D3, D5, and D10 were 9.6, 10.9, 8.0, and 9.5, respectively.

After the QPS detected the quench in D3, the protection heaters were fired causing the two outer coils to quench, finally followed by the lower inner coil quenching from outer coil thermal diffusion with a similar progression occurring for D10. Magnets D7 and D8 quenched after the QPS detected the initial D6 quench and fired all protection strip heaters in that quarter cell, just as D1 and D2 (D9 and Q2) were quenched by protection heaters after the quench was detected in D3 (D10). The progression of induced quenches is consistent with the single magnet test data since D10 had shown a similar but reduced ramp rate sensitivity compared to D1, D2, and D3, but was significantly more sensitive than D9. The explanation for these quenches is that the reduction of inductance in the string occasioned by the quenching of the third quarter cell (D6 location) resulted in a down ramp sufficiently rapid to cause a ramp rate induced quench in the first quarter cell (D3 location) but not the fourth (D10 location). However, once the inductance of the first and second quarter cells was also effectively removed by the activation of the bypass circuit during their quenching, the resulting down ramp increased sufficiently to induce a quench in D10.

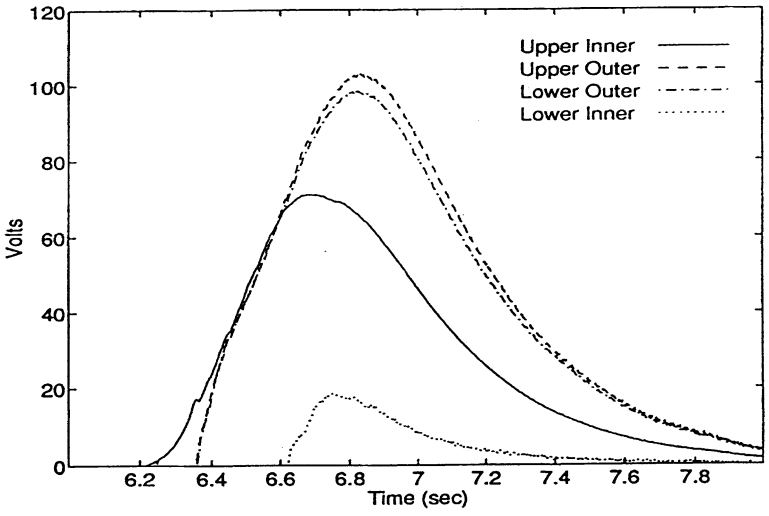

FIGURE 10: A plot of the most resistive element in each of the protection units as a function of time for the 6500 A strip heater induced quench in which the first and fourth quarter cells quenched due to and excessive down ramp rate.

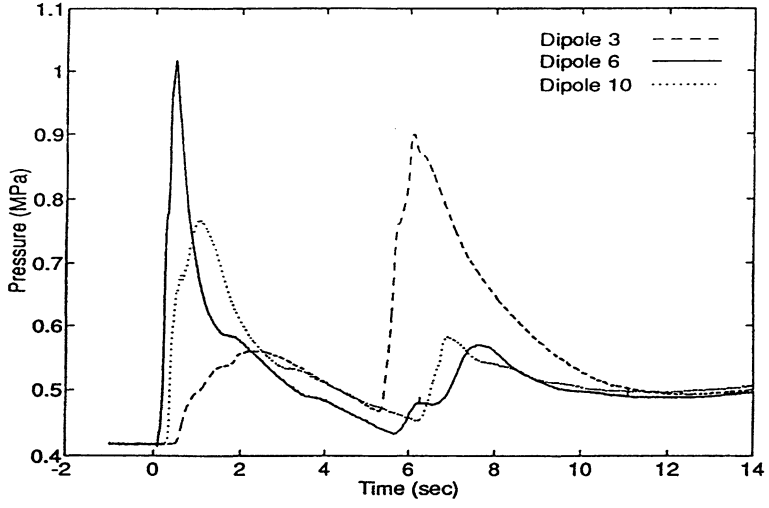

FIGURE 11: A plot of the dipole end bell cold pressure transducer's output as a function of time is shown for the same 6500 ampere strip heater induced quench in D6 as Figure 9. Note that the pressure peaks occurred well before the secondary quenches occurred.

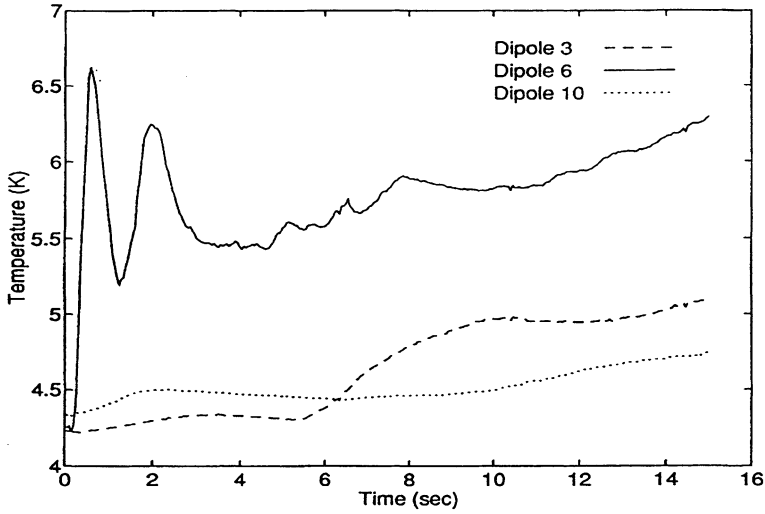

FIGURE 12: A plot of the dipole end bell thermometer output as a function of time is shown for the same 6500 ampere strip heater induced quench in D6 as in Figure 9.

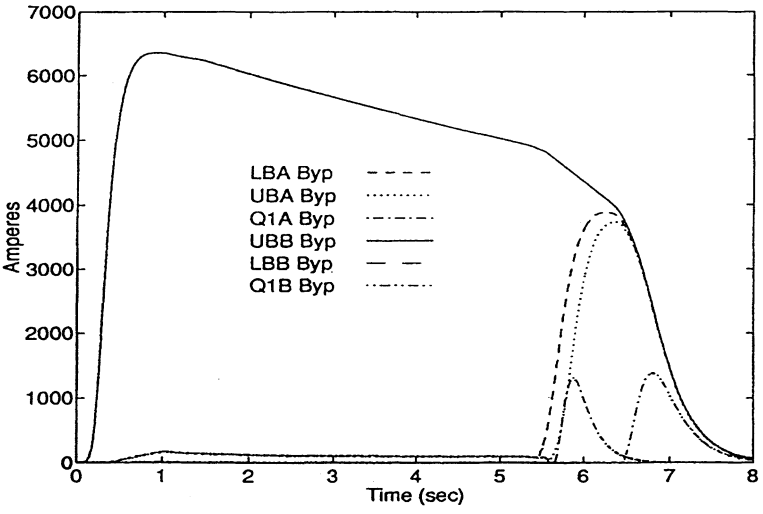

FIGURE 13: The current profiles through the bypass circuits for the same 6500 A strip heater induced quench in D6 as in Figure 9 where zero time is the time at which the strip heaters were activated.

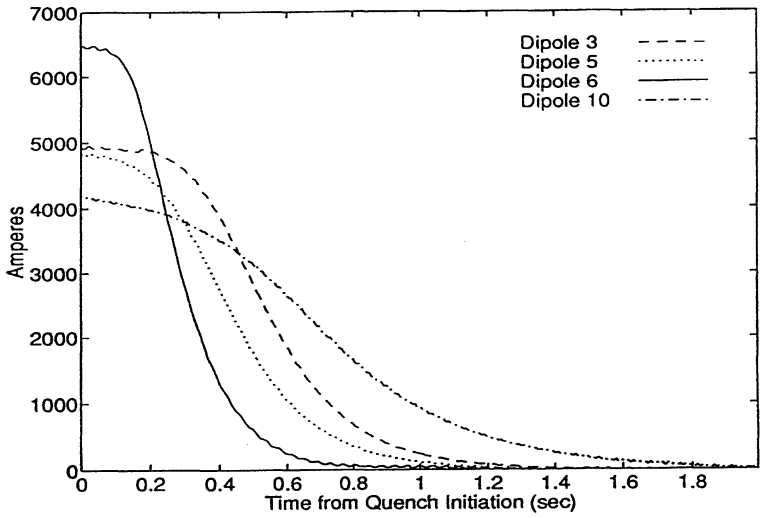

FIGURE 14: The current profiles through the magnets for the same 6500 A strip heater induced quench in D6 as in Figure 9 where zero time is the time at which the strip heaters were activated.

Temperature and pressure data acquired during this event is consistent with the interpretation of D3 and D10 quenching because of ramp rate induced heating and not from helium heated by the quenching of D6, D7, and D8. Data presented in Figure 11 shows the coldmass pressure history for this event for dipoles 3, 6, and 10. The initial increase in the helium coldmass pressure due to the quenching of the third quarter cell reached D3 at ~0.3 seconds and D10 at ~0.5 seconds. After these times, helium heated by the original quench is present in the dipoles. However, the data in Figure 12 shows that the temperature rise from the heated helium is not sufficient to initiate a quench. The temperature sensors in the dipole cold masses are located such that they would detect a temperature increase due to heated helium, but not an increase in coil conductor temperature due to ramp rate induced heating. Thus, a rise in temperature above the maximum superconducting temperature in these magnets is not evident until the protection heaters are fired causing a large volume of the magnet to quench. The delay in the quenching of the lower inner coils would almost certainly have been significantly less if the quenching of the upper inner coils of dipoles 3 and 10 had been due solely to the presence of heated helium. Furthermore, note that if the quench data of D10 (DCA212) versus temperature is extrapolated[19] then the critical current for the quench is 7300 amperes at 4.3 K with a slope of 1550 amperes/degree Kelvin would lead to critical temperatures as follows: 5600 amperes-T_c = 5.6 K; 4700 amperes-T_c = 6.3 K; 3700 amperes-T_c = 7.0 K.[22]

It is also important to note the response of the string bypass circuits during this event. Although all the magnets in the string were eventually quenched, only five of the six bypasses conducted current. The bypass protecting dipoles 9, 10 and Q_2 did not engage due to competing voltages electrically upstream and downstream from this quarter cell not

TABLE 5: Strip heater induced quenches propagating from cell "B" to "A".

Event	$\sim T_{D3}$(K)	I_{max}	t_Q(S)	I_Q(A)	$<dI/dt$(A/S)$>$
D6	4.24	6500	5.07	4960	–307
Half Cell	3.99	6600	3.03	5420	–392
Half Cell	3.95	6600	3.10	5400	–390
Half Cell	4.45	6600	5.97	4718	–295
D8	4.45	6700	3.08	5620	–382
Half Cell	4.45	6700	4.12	5305	–319

allowing enough bias voltage to develop for the bypass diode to begin conducting current. The high MIITS experienced by D10 can be attributed to the absence of the bypass in removing current from that quarter cell, thus allowing a long current decay through the magnet. The bias voltage in this circuit would have been increased by the presence of a greater number of magnet cells, but the MIITS value would probably have still been high relative to the quenching current. The current through the bypass circuits is shown in Figure 13. The current decays through the dipoles are shown in Figure 14 where it is evident that the relatively long decays of D3 and D10 compared to D6 resulted in the unexpectedly high MIITS of the secondary quenching magnets.

A total of six initiating events were observed to produce ramp rate induced quenches during Run 3. In each event the first magnet to quench because of ramp rate induced heating was D3 in the first quarter cell, and the second quarter cell was quenched by the protection heaters due to the QPS declared relative dI/dt failure. The "dI/dt failure" was a calculation error discussed previously. Four of the six events were quenches induced in the entire second half cell by simultaneous activation of all twelve protection heater circuits. The other two events were initiated by firing a protection strip heater in D6 (discussed above) and a spot heater in D8. During the D8 spot heater event, the fourth quarter cell was quenched due to a relative dI/dt failure, and not because of a ramp rate induced quench in D10. Data summarizing these six events are presented in Table 5.

The solution attempted to prevent the occurrence of a ramp rate induced quench was to decrease the value of the dump resistor in order to increase the L/R time constant. This worked for events initiated in a single quarter cell, but not for the simultaneous quenching of the second half cell. For example, as noted in Table 5, the average dI/dt experienced by D3 in the five seconds before it quenched was approximately -330 A/s in the D6 strip heater event discussed above. Immediately after that event, the dump resistance was decreased from 0.022 ohms to 0.012 ohms, and another 6500 A strip heater quench was initiated in D6. The increased time constant resulting in an average down ramp rate of about -230 A/s which did not cause a ramp rate induced quench. The quench was confined to the third quarter cell. A comparison of the down ramp for these two events is shown in Figure 15. After the realization that the dump resistor could be used to successfully confine quenches in a single quarter cell, quench containment became a straightforward matter although it was not possible to contain a full half cell B quench. This was because the cabling in the dump circuit contained enough resistance to cause a down ramp fast enough to quench D3.

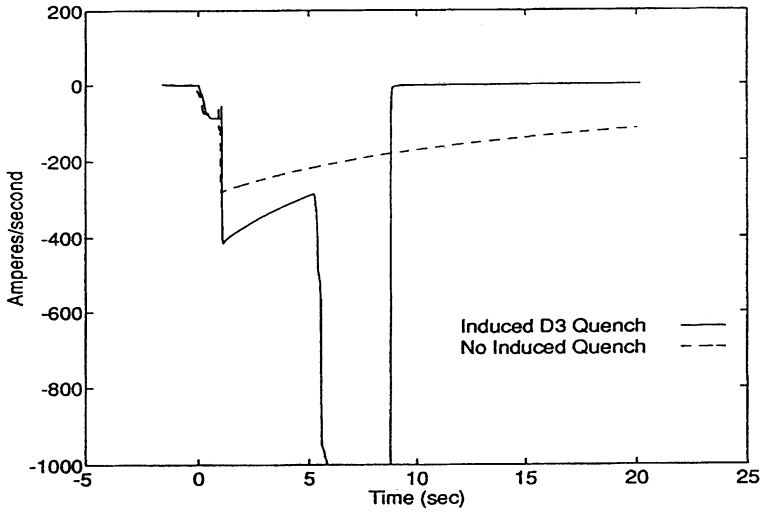

FIGURE 15: The down ramp rate profiles are shown for two D6 strip heater 6500 ampere events, one of which led to an induced quench in D3 (solid line), and one of which did not because the dump resistor reduced value increased the L/R time constant past the critical value (dotted line).

Evidence to support this was that full half cell A quenches were easily contained because the down ramp rate did not exceed the minimum needed to quench D6 or D10. The one ramp rate induced quench in D3 that occurred during the D8 spot heater tests occurred at a current of 6700 A and a dump resistor value of 10 mohms. Prior to that test, spot heater quenches in D8 had been carried out at currents up to 6500 A without a D3 ramp rate induced quench. Subsequent to that quench, the dump resistor value was lowered to 5 mohms, another 6700 A D8 spot heater quench was initiated, and the quench was confined to the third quarter cell.

There were two other events in addition to those involving ramp rate induced quenches in which the entire cell eventually quenched. During these two events, a weakness in the QPS threshold detection algorithm or the relative dI/dt failure caused heaters to fire in quarter cells other than the one in which the original quench was initiated. The weakness in the detection algorithm was that at the time a heater was fired in a magnet, inductive responses in other magnets could momentarily mimic the presence of a small resistive voltage that exceeded the detection threshold. The detection threshold was set to 1.0 volt to alleviate this problem. As shown in Table 6 for these eight events, one of the six bypass diodes did not develop enough bias voltage across it to conduct current. This is a weakness in the QPS design. The problem might not be as severe when a greater number of magnet cells are present, but nevertheless, needs to be addressed in future accelerators where this QPS concept is used.

If one accepts the explanation for the inner coil quenches as being due to ramp rate induced heating of the coil windings past the critical temperature, then it is possible to use

TABLE 6: Current bypass segments conducting by event type.

Event Type	I_{max}	LB-A	UB-A	Q1	UB-B	LB-B	Q2
D7 Strip Heater	5500	N	Y	Y	Y	Y	Y
D6 Spontaneous	6347	N	Y	Y	Y	Y	Y
D6 Strip Heater	6500	Y	Y	Y	Y	N	Y
Half Cell B	6600	Y	N	Y	Y	Y	Y
Half Cell B	6600	Y	N	Y	Y	Y	Y
Half Cell B	6600	Y	N	Y	Y	Y	Y
D8 Spot Heater	6700	Y	N	Y	Y	Y	Y
Half Cell B	6700	Y	N	Y	Y	Y	Y

the down ramp data obtained during Run 3 to estimate the maximum sustainable energy loss density in the inner coil windings. Losses due to both magnetization and ramp rate dependence have previously been computed from data obtained in up ramp tests conducted at the FNAL Magnet Test Facility (MTF).[23–25] Using the MTF results to estimate losses in the magnets during an ASST quench, it is possible to calculate that the magnets most sensitive to induced heating (dipoles 1, 2, and 3) could sustain a load of 7.3 watts/meter of magnet length without quenching during a down ramp, but they could not sustain a load of 10.5 watts/meter of magnet length.

4.3 Magnet operating margin

The two spontaneous quenches that occurred during commissioning were at currents of 5977 and 6347 amperes for D10 and D6, respectively. These currents are greater than 90% of the peak designed operating current. Both of these quenches arose in the lower inner coils of the dipoles with the quarter coil resistive voltages for these events shown in Figures 16(a) and 16(b). Although the cause of the spontaneous quenches cannot be precisely determined, it is possible that they were training quenches resulting from thermal cycling. Dipole DCA316 (D6) had been run in the half cell tests without quenching spontaneously; however, it had experienced two training quenches during its single magnet tests at FNAL, whereas the other Fermilab dipoles used in the ASST had experienced either zero or one training quench.[14,15] Dipole DCA212 had been involved in a maximum MIITS test at BNL prior to its installation in the ASST that raised the measured coil temperature above 735 K (a measured value with the calculated MIITS being 20.06).[26,27] Thus, the spontaneous quench in this magnet could have resulted from the extreme conditions it underwent during that experiment. The peak voltage magnitude differences are consistent with the peak current differences. These voltage profiles were similar to those observed in the 40 mm aperture half cell spontaneous quenches but at lower currents.[28,29]

The full cell was twice taken to currents in excess of 6900 amperes in order to further investigate the operating field margin of the magnets. A power supply software over-current trip occurred on the first attempt activating the dump circuit and ramping the string down without a quench. On the second attempt, the string was taken to a current of 7035 amperes,

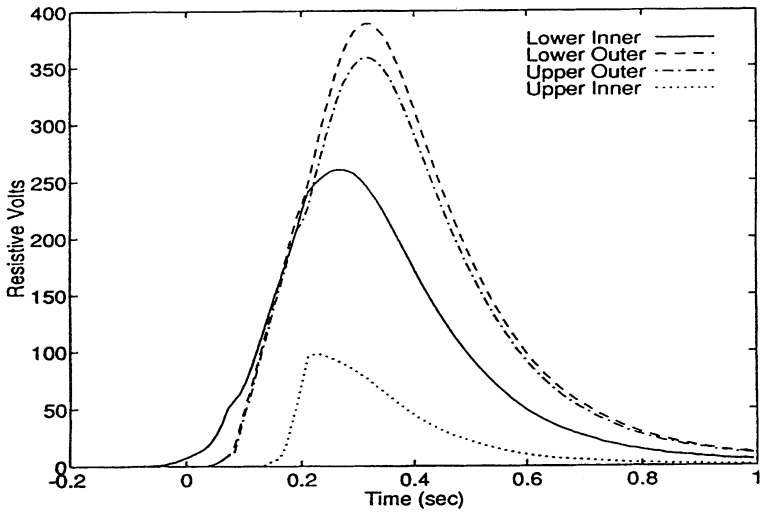

(a)

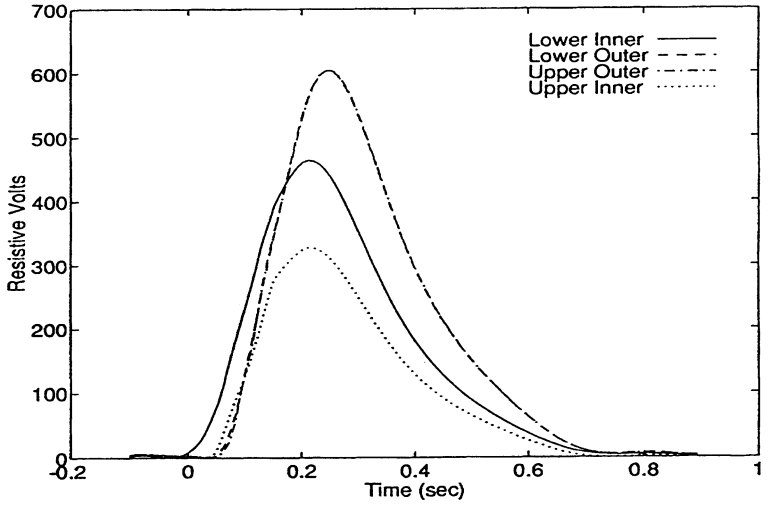

(b)

FIGURE 16: These resistive voltage profiles as a function of time for the two spontaneous quenches observed during the ASST testing are quite similar. Figure 16(a) profiles are for D10 (DCA212) for the spontaneous quench at 5977 amperes. The Figure 16(b) profiles are for D6 (DCA316) for the spontaneous quench at 6347 amperes. The peak voltage magnitude differences are consistent with the current differences seen in the spot heater induced quenches at different current levels. These profiles were similar to those observed in the lower current spontaneous quenches in the 40 mm aperture half cell.[27,28]

held there momentarily, and a spot heater induced quench was initiated in D10. This quench was successfully contained within the fourth quarter cell. The peak pre-quench temperature along the string was 0.24 K less than the maximum magnet design operating temperature of 4.35 K during this test. As expected, the highest MIITS value observed during the full cell tests occurred during this quench with a value of 13.5, corresponding to a maximum adiabatic quench origin temperature in the outer coils of 431 K.

4.4 Strip heater design comparison

A series of seven strip (protection) heater induced quenches was conducted to study the quench response of the magnet to three different heater designs.[18] The dipole magnet heater protection consists of two heater circuits each containing two heater strips.[30] Each strip possesses twelve stainless steel heater pads spaced at roughly equal intervals along the 15 meter copper strip length. The pads are 1.27 cm wide and 25.4 microns thick. The heater design parameters are the same for the three designs with the exception of the pad length. The standard design used in all the dipoles has 61 cm long pads while the two experimental designs have pad lengths of 5 cm (DCA322) and 10 cm (DCA323). Dipoles DCA322 and 323 each contained one circuit with the standard heaters and one circuit with the experimental heaters. The experimental designs (low energy heaters) reduced the required energy to reach a given temperature by up to an order of magnitude compared to the standard design (high energy heaters). Quenches were induced in DCA322 (D5) and DCA323 (D4) using either the standard or experimental designs at low (3000 A) and high (6000 A) cell currents. The energy delivered to the heater circuits had previously been adjusted to give approximately the same thermal diffusion time from heater firing to quench onset in the outer coil windings. This adjustment was made to produce coil resistance in less than 250 ms at 2000 A with typical times of 150–200 ms observed during the initial 2000 A commissioning quenches.

The data from this study demonstrates the importance of the electrical circuit characteristics of the strip heaters in QPS design. There are two thermal time scales affecting the delay from heater firing to quench onset: the time constant of the RC heater circuit and thermal diffusion of the heat through the magnet insulation. The time required for the heat to develop in the high energy heaters to initiate a quench at low magnetic field ($\sim 3T$) was slightly less than the time for the low energy heaters. However, the relationship reversed by the time the magnetic field reached $6T$. Figure 17 clearly shows that the experimental designs use much less energy than the standard design, but it is not clear from this figure why the quench times for the 6000 A quenches were less for the low energy heaters. The reason is made evident, however, in Figure 18, which plots the integrated energy density, rather than the total integrated energy, as a function of time. An approximate adiabatic temperature of the heater pads has been calculated from the energy density and physical characteristics of the stainless steel pads although the actual pad temperature will be somewhat less due to the very large volume of dense solid material of the coil in close contact with the heater strip. The much faster rise time of the new low energy heater design results in the quench delay being only a function of the thermal diffusion constant of the insulation. The data collected during this study is consistent with that obtained during special single magnet tests at FNAL.[31,32] Moreover, the data presented here when compared to the delay times

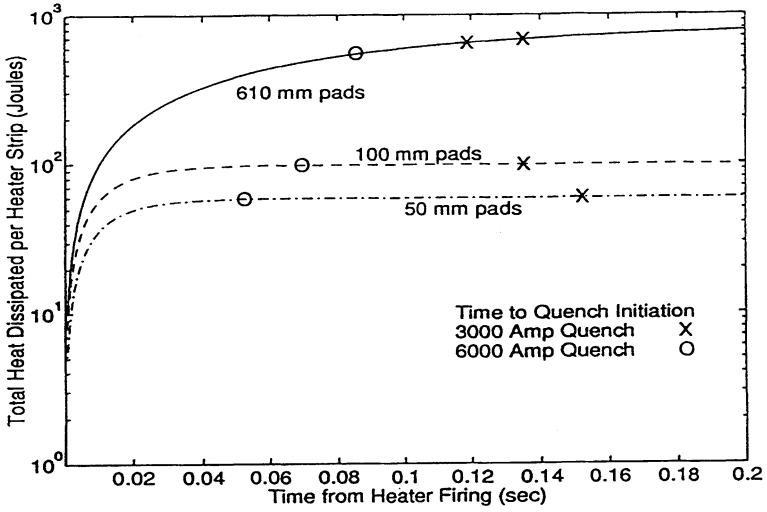

FIGURE 17: The total energy absorbed by a heater strip after activation for experimental and standard heaters is plotted.

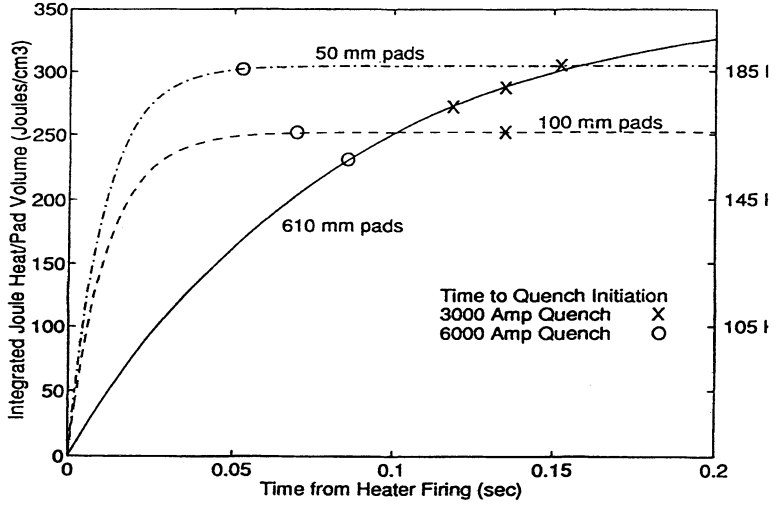

FIGURE 18: The energy density as a function of time for the standard heaters and experimental heaters with their adiabatic temperature shown on the right corresponding to a given energy density in stainless steel.

TABLE 7: Spot heater induced quench data for selected magnets.

I_{max}(A)	T_{feed}(K)	T_{end}(K)	MIITS	VTG_{max}	VTG_{min}	Coil V_{max}	Coil V_{min}
			Magnet D8				
4793	4.250	4.52	7.0	112	–69	134	–456
5000	4.25	4.51	12.2	118	–85	150	–102
5500	4.25	4.53	12.5	79	–45	96	–84
6000	4.00	4.33	12.8	75	–46	66	–74
65000	4.19	4.50	11.6	33	–274	284	–245
6700	4.19	4.49	11.9	38	–478	376*	–281
6700	4.00	4.40	11.7	30	–231	261	–248
			Magnet D10				
5000	4.01	4.31	12.2	152	–33	33**	–28
6000	4.01	4.33	12.9	112	–46	123	–101
6700	4.17	4.47	12.2	196	–80	273	–190
7000	3.82	4.11	13.5	328	–111	378	–313

*Values given are for the third quarter cell (containing D8), the minimum and maximum voltages, for the event occurred in the fourth quarter cell.

**Values given are for the fourth quarter cell (containing D10), the minimum and maximum voltages, for the event occurred in the third quarter cell.

in Tables 2 and 3 along with the critical temperature versus quench current referred to in Section 4.2, give a reasonable understanding of the critical quench initiation parameters, i.e., 6000 amperes corresponds to 5.3 K (T_c) and 3000 amperes corresponds to 7.6 K (T_c) roughly.

4.5 Spot heater quenches

A series of spot heater induced quenches was conducted at various magnetic fields in order to simulate localized spontaneous quench conditions. These types of resistive transitions typically lead to higher MIITS values than for strip heater quenches.[33] Due to the severe time limitations of performing as many experiments as possible within the allotted time period, it was not possible to characterize magnet and string behavior as fully for the spot heater quenches as was possible for the strip heater quenches. For example, since it was necessary to gain as much information as possible about refrigerator and string performance and capability at different string operating temperatures, the temperatures were different for many of the spot heater events. Thus, it is not possible to present a meaningful MIITS vs. current plot as the MIITS is a sensitive function of the operating temperature (cf. the lower limit of the MIITS integral). However, a summary of the electrical data for spot heater induced quenches is presented in Table 7, and shows, as expected, that the MIITS values are higher and the maximum voltage-to-ground values are lower compared to quenches induced with strip heaters. These differences are probably due to differing coil volumes and distributions involved in the quench initiation and development.

The initial events of this series were used to verify that the spot heaters were delivering at least the minimum energy required to initiate a quench. During the first of these tests, a delayed protective measure was employed where the QPS automatically fired the protection heaters approximately a hundred milliseconds after the spot heater. This operation was discontinued after it was verified that the spot heaters were indeed inducing a quench, and the protection heaters were subsequently fired only after the QPS detected quench onset in a half coil. This was the planned designed operational sequence of the QPS for the Collider.[21,34,35] The series was concluded with the spot heater quench in D10 at 7035 A, corresponding to a $7T$ magnetic field, well above the required field of $6.5T$ for 20 TeV operation (see Section 4.3).[36]

4.6 Test of the half cell bypass circuit

In order to assess the feasibility of reducing the number of QPS protection units by increasing the number of magnets within a protection unit, the full cell was reconfigured to place the upper buss magnets (D4, D5, Q1, D6, D7, and D8) into a single half cell bypass circuit. This was achieved by disconnecting the upper buss bypass lead at the SPR, and appropriately modifying the QPS logic. Before actually disconnecting the bypass lead, the software changes to the QPS were tested with a 5500 A strip heater quench of D7. This check ensured that the protection strip heaters in all the magnets in that half cell would fire simultaneously once a quench was detected in it. After the physical change to the bypass circuit was made, quenches of 3000 A and 5000 A were initiated by strip heaters in D6. The QPS functioned normally in detecting the quench and protecting the magnets by firing the protection heaters. However, observed voltages-to-ground were higher than acceptable for normal operations. One contributing factor to the high voltages is clear from a plot of the dipole resistive voltages shown in Figure 19 for the first 0.4 seconds of the 5000 A quench: because of the apparently different quench initiation times in the dipoles, the voltages grow similarly to the situation in a half cell with unmatched RRR dipoles.

A possible reason for the differing quench times is that D4 and D5 are upstream and D6, D7, and D8 are downstream from the mid-cell spool recooler. A second and probably more dominant factor is that the entire cell temperature was about 0.5 K colder than the nominal 4.35 K operating temperature used for most of the testing. The lower temperature resulted in a longer delay for the protection heaters to become effective. From Table 3, at 5000 A there was a 55 ms heater delay from strip heater firing to the detection of one resistive volt in a D5 half coil at 4.35 K. However, in the strip heater induced quench in D6 for the five dipole protection test, this delay increases to 135 ms at 3.8 K. The additional delay represents an increase of at least 425 volts to 475 volts. By reducing the heater response time to 55 ms, this increase in voltage can be reduced to the 900 to 1000 volts range at 5000 amperes. This is high but probably tolerable in normal operations. The other factor to be considered is the volume of the coil driven normal by the protection heaters, which could be increased by redesigning the strip heaters. This may or may not reduce the voltage until all of the outer winding is driven normal, but it would then be a simple matter to reduce the delay between recognition and the quenching of the remaining magnets in the protection unit by balancing the heater energy density, time constant, and QPS threshold.

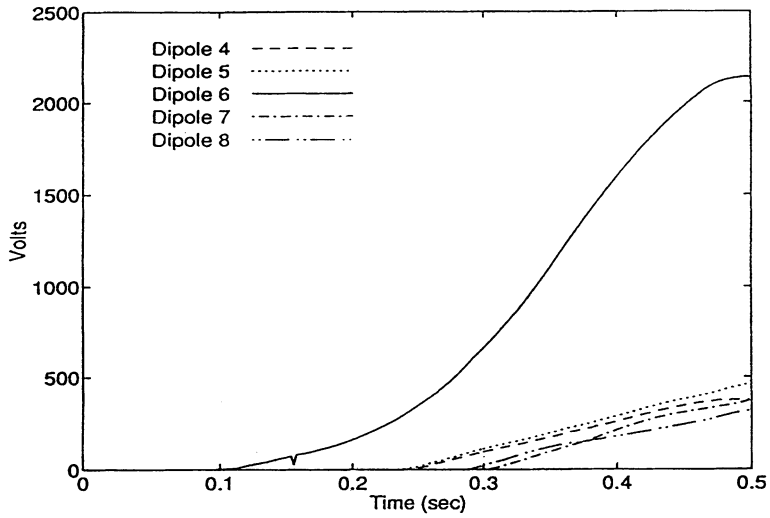

FIGURE 19: The voltage profiles for the upper buss dipoles are plotted as a function of time and clearly show that the initiating magnet took off almost 150 milliseconds ahead of the rest of the magnets resulting in large differential voltages being developed.

It should also be mentioned that the first quarter cell quenched, but not the fourth, for both the 3000 A and 5000 A events. The reason for this is a weakness in the QPS detection threshold algorithm as discussed at the end of Section 4.2. In these cases, a negative voltage induced in D4 and D5 in response to the protection heater being fired in D6 resulted in a positive inductive voltage in D1, D2, and D3 that exceeded the 1.0 volt threshold. The detection of this "false quench" resulted in the activation of the protection heaters in the first quarter cell.

4.7 Degradation of the insulation vacuum

The last experiment performed during Run 3 was to degrade the insulation vacuum in the second half cell in a controlled fashion to mimic a catastrophic failure. This type of test has not been performed previously on actual systems because of the possible risk to equipment and string components. However, because of the SSC termination, the ASST string was basically expendable, and it was decided that the importance of collecting data on this phenomenon outweighed the risks. Both helium and air leaks are possible sources of vacuum degradation, but time constraints allowed using only air as a degradation source as its impact was thought to be more severe.[37]

The insulating vacuum between the two half cells was isolated by a vacuum barrier in the SPR spool. To degrade the insulating vacuum, air was admitted by opening an electrical gate valve (2.54 cm aperture) located at the D6-D7 interconnect. The gate valve aperture was restricted by an orifice consisting of a 15 cm long, 0.95 cm ID tube. The string was

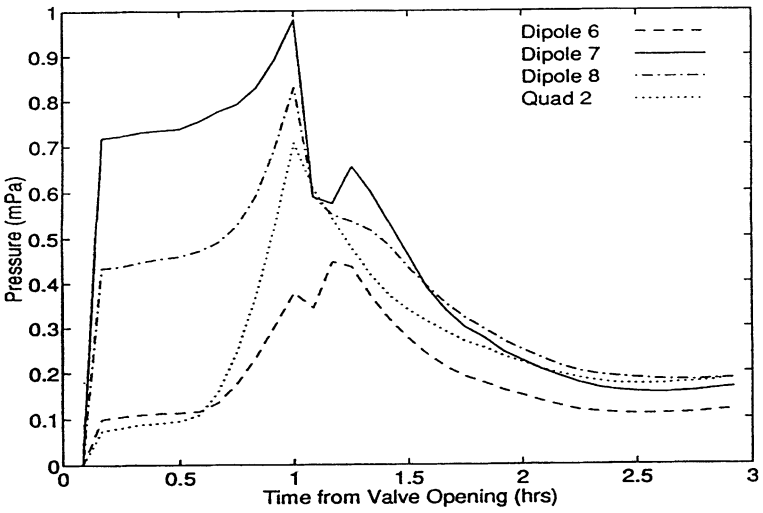

FIGURE 20: The insulating vacuum pressure in the second half cell after the opening of the vacuum gate valve to the atmosphere.

isolated from the refrigerator prior to the test for safety reasons. The valve was opened for approximately 54 minutes, and data was collected during this time on three data acquisition systems at rates ranging from 3.3 MHz to several hundred hertz. At the peak cold mass pressures, the LHe return line safety valve, set at an opening pressure of 0.95 MPa, was opened and vented cold gas. The valve cycled several times during the 54 minute test. The standard data logging system continued to record data at 5 minute intervals during the warm-up process. The insulating vacuum was restored with vacuum pumps after test completion.

The data from the test clearly shows that the system did not suffer from this type of catastrophic failure, and, in fact, the response was rather benign. Figure 20 shows the response of the insulating vacuum to the presence of the leak as a function of time. Figure 21 shows the pressure response at the two ends of the string as well as the temperatures from selected dipoles along the string, and Figure 22 shows the temperatures of the 4 K, 20 K, and 80 K lines for dipole 7. The observations are not in agreement with failure response models used for safety design calculations that predicted catastrophic results.[37] The experiment should be repeated with helium which would not have frozen out between layers of MLI as did the air which was the explanation for the self-limiting behavior.

4.8 Quench pressure data

The pressure data obtained during magnet quenches indicates that the quench relief valves operated properly, and did not allow the helium pressure in the cold mass to reach a level that could adversely affect the cryogenic integrity of the string. The maximum quench pressure

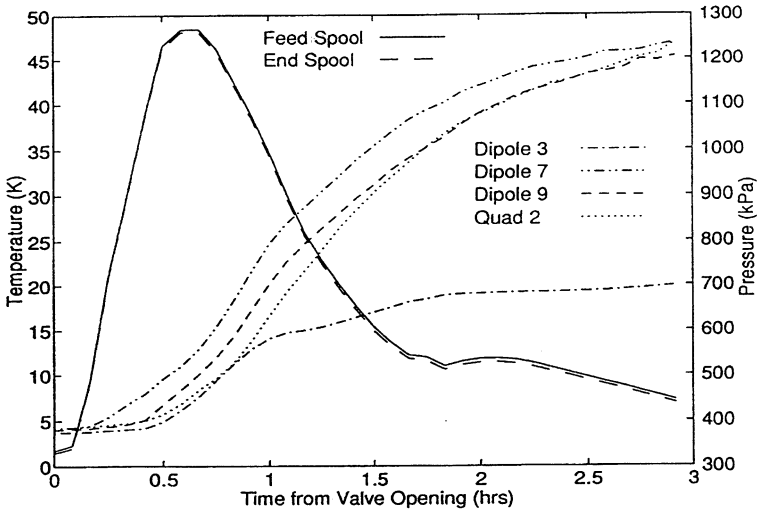

FIGURE 21: The time profiles of the pressure of the cold mass circuit at the feed and end spools. Note the rather slow build up of the pressure. Also shown are the cold mass temperatures as measured in the end bells of the various magnets. These are referenced again to the opening of the valve which spoiled the insulating vacuum in the second half cell magnets D6, D7, D8, D9, D10, and Q2 plus the end spool only. Note the very slow increase in temperature of the first half cell: the temperature at D3 (DCA315) was only about 20 K after 3 hours.

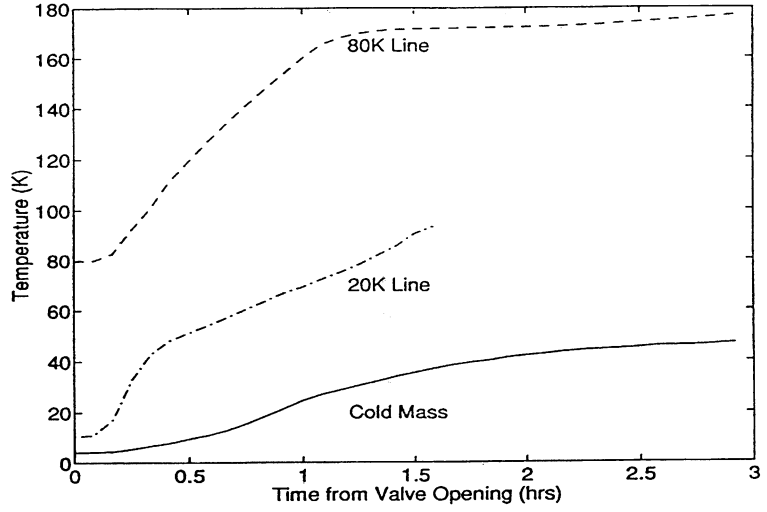

FIGURE 22: These are temperature histories of the various cryogenic circuits in the D7 interconnect nearest to where the valve was located that was used to spoil the insulation vacuum. It is clear when the valve was closed again 54 minutes later.

observed during Run 3 was 1.3 MPa, and occurred during a D8 spot heater induced quench. During the safety certification process of the string, the cold mass, liquid helium return, and 20 K helium shield lines had been successfully tested at a static pressure of 1.85 MPa.

It is interesting to compare the maximum pressure observed in a half cell during strip heater induced quenches as a function of current as presented in Table 8. From this data it is evident that the pressures are approximately the same whether the quench was initiated in half cell A or B. Some of the higher maximum values observed in the second half cell pressures when compared to the first half cell, and the higher pressure values for quenches originating in the third quarter cell compared to those of quenches of the entire second half cell, are possibly due to the quench valves' logic opening response. The logical response was determined by the quench location. Only the valve in the feed (end) spool is opened for quenches located in the first (fourth) quarter cell, while the valve located in the SPR is opened for quenches located in the second and third quarter cell. The quench pressure front from the third quarter cell had to pass through the heat exchanger to reach the SPR quench valve while that of the second quarter did not. In addition, the valve in the feed spool was to be found to open more quickly than the valve in the end spool. An examination of all the pressure data indicates that the maximum pressure occurring in a dipole is independent of the initiating event type (strip or spot heater induced or spontaneous), but depends only on the firing of one or both sets of strip heaters.

In order to compare the results from different types of quench events, Figure 23(a) plots the pressure data for a 6500 A strip heater induced quench in dipole 3, Figure 23(b) shows the 5977 A spontaneous quench pressure data in dipole 10, and in Figure 23(c) the pressure data for the 7000 A spot heater induced quench in dipole 10 is shown (all three quenches were confined to a quarter cell). Note that the pressure curves in Figures 23(b) and 23(c) are virtually identical in shape showing that the spot heater induced quench mimics spontaneous quench thermodynamic conditions quite closely; the difference in peak magnitudes can be ascribed to the different quench currents. Also note the change in slope of the pressure decays at $\sim$3 seconds in Figures 23(a), (b), and (c), correspond to the heating of residual liquid helium in the magnet cold masses. This interpretation is supported by a numerical model of the magnet string cryogenic system as discussed in Reference 38. Finally, as shown in Figure 24, it is possible to use the data from strip heater induced quenches in the first half cell to calculate the speed of the original pressure wave as it travels through the second half cell.

5 HEAT LEAK MEASUREMENTS AND RESULTS

The heat leak measurements for the full cell configuration of Run 3 were conducted prior to the power testing during September and October 1993. The data collected during Run 3 is consistent with the half cell measurements and seems to indicate that the heat leak into the magnet cold mass is approximately three times higher than the design budget, the heat leak intercepted by the 20 K shield is approximately the design value, and the Run 2 measurements indicate that the heat leak intercepted by the 80 K shield is substantially under budget.[8] No 80 K heat leak measurements were obtained for the full cell run due to a lack of stability in the new string LN_2 system. The heat leak data is summarized in Table 9.

TABLE 8: Peak pressure data for different quench event types.

Initial Magnet	I_{max}(A)	Meas. Pt.	P_{max}(MPa)
Half Cell A — Peak Pressures for Strip Heater Events			
D5	5000	D5	0.689
D3	5000	D1	0.814
D5	5500	D5	0.765
D2	5500	D2	0.827
D3	6000	D2	0.910
D5	6000	D5	0.869
D5	6500	D5	0.972
D3	6500	D2	0.986
Half Cell B — Peak Pressures for Strip Heater Events			
D7	5000	D6	0.814
D7	5500	D6	0.917
D7	6000	D6	0.931
D6	6500	D6	1.020
D6	6500	D7	1.103
D9	6600	D10*	0.793
Full Half Cell Quenches — Peak Pressures			
HCA–D5	6600	D3	1.138
HCB–D7	6600	D7	1.193
Spot Heater Quenches — Peak Pressures			
D8	5000	D7	0.972
D8	5500	D7	1.273
D8	6000	D7	1.131
D8	6500	D7	1.241
D8	6700	D7	1.296
Standard and High Efficiency Heater Tests			
D4	6000	D5	0.889
D4	6000	D5	0.876
D5	6000	D5	0.848
Five Magnet Protection Cell Test			
D6	3000	D7	0.655
D6	5000	D7	0.979
Spontaneous Quench Data			
D10	5967	D10	0.765
D6	6347	D8	1.062

*The D9 pressure sensor was broken.

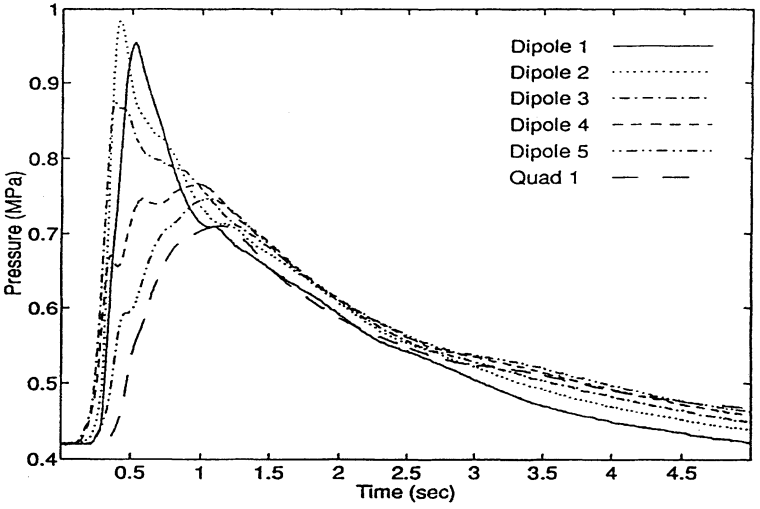
Dipole 1
Dipole 2
Dipole 3
Dipole 4
Dipole 5
Quad 1
Pressure (MPa)
Time (sec)
1
0.9
0.8
0.7
0.6
0.5
0.4
0.5
1
1.5
2
2.5
3
3.5
4
4.5

(a)

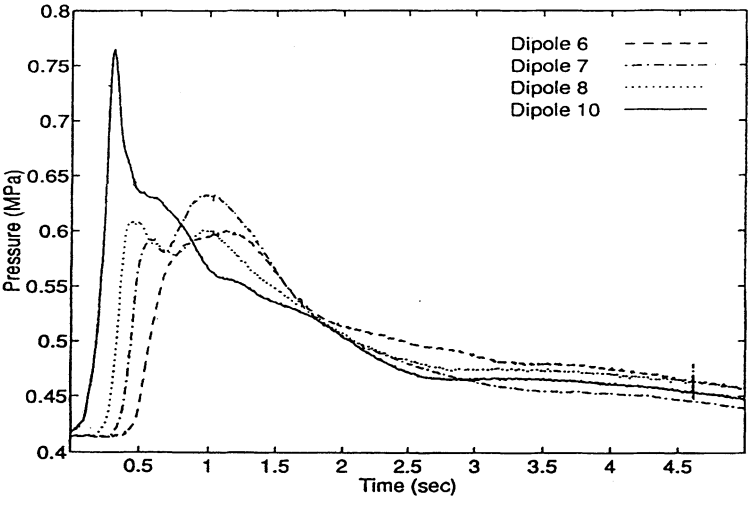
Dipole 6
Dipole 7
Dipole 8
Dipole 10
Pressure (MPa)
Time (sec)
0.8
0.75
0.7
0.65
0.6
0.55
0.5
0.45
0.4
0.5
1
1.5
2
2.5
3
3.5
4
4.5

(b)

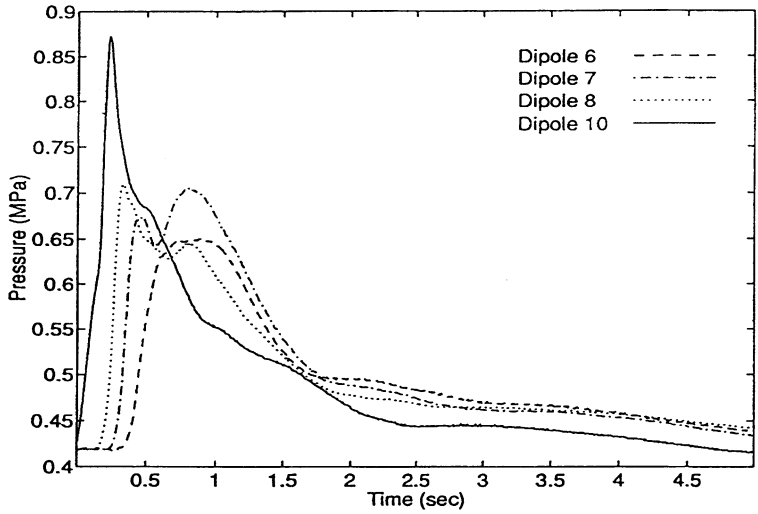

(c)

FIGURE 23: These pressure profiles as a function of time measured with the cold pressure transducers in the end bells of the cell magnetic elements are shown for three differently initiated quenches. Figure 23(a) is for a protection strip heater induced event at 6500 amperes in D3, Figure 23(b) is for a spontaneous quench in D10 at 5977 amperes and Figure 23(c) is for a spot heater initiated quench in D10 at 7035 amperes. Note that all the quenches were contained within a protection unit (quarter cell). It is of special interest to compare the similarities of Figures 23(b) and 23(c).

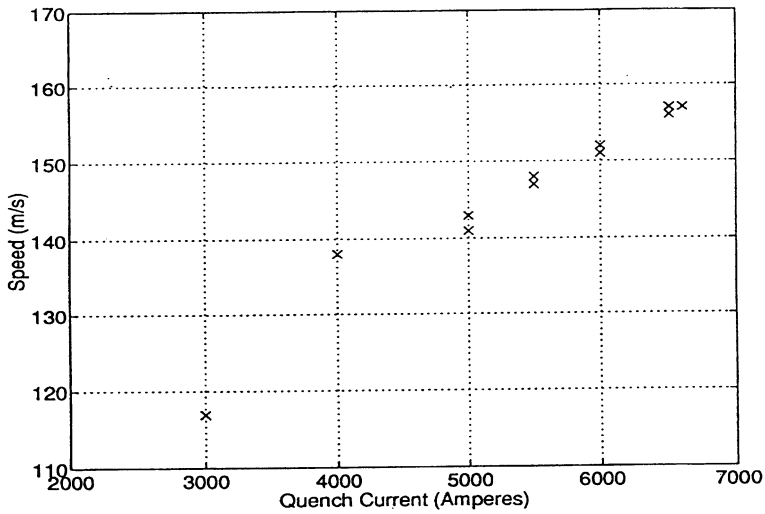

FIGURE 24: The speed of the pressure wave front generated by a strip heater quench is plotted as a function of the magnet current.

TABLE 9: Thermal heat leak results.

Circuit	Run 1	Run 2	Run 3	Budget
	Average Heat Leaks for Dipoles Plus Interconnect in Watts			
Cold Mass, 4K	1.3±33%	1.4±28%	1.25±33%	0.36
20K Shield	NA	5.59±10%	5.4±10%	5.06
80K Shield	28.0±14%	24.5±16%	NA	37

The analysis of the thermal data presented in this table was complicated by the various running configurations used during the collection of thermal data. The data above represents the heat leak results when the 4 K, 20 K and 80 K circuits were near nominal operating temperatures. That is, the 80 K shield was maintained between 80 K and 90 K, the 20 K shield was between 20 K to 27 K and the cold mass operated between 3.8 K to 4.5 K. Due to the very high heat loads of the feed, end, and SPR spools, the cold mass and 20 K circuit loads were determined using only the interior 3 dipoles in the first half cell. The measurements on the units next to the spools were always affected by the high adjacent loads. For example, the quadrupoles always appeared to have a high heat load which varied greatly: Q1's 20 K shield appeared to have a 6.7 watt load while Q2's 20 K shield load measured 13.9 watts. The heat load profiles down the string were the lowest in the middle of the half cells, and rapidly increased in the vicinity of the spools. The calculation technique employed to determine the heat loads was checked by powering internal calibration resistors placed in the various circuits during the string assembly. This provided a calibrated heat load to the string. When the measured increase in temperature was combined with the measured mass flow rate, the calculated heat load agreed to the test electrical loads used to within ±4%. The mass flow sensors were checked by comparing the measured values using the manufacturer calibrations to a room temperature gas volume meter. The values agreed to better than 10%. However, due mainly to the large heat leaks from the spool pieces, the Run 3 thermal data has not provided more accurate information beyond that obtained from the Run 2 measurements.[6]

6 CONCLUSIONS AND DISCUSSIONS

The results of the full cell prototype string test were very satisfactory in that several of the original goals set for the run were achieved. Arguably one of the most crucial questions was whether the previously observed voltages-to-ground could be reduced by matching the low temperature normal state resistance of the dipole outer coil windings within a protection unit. This matching was achieved at the 10% level, and the resulting reduced voltages were within the desired operation range of less than two kilovolts. Of course, there are several factors that ultimately affect the voltage of the magnets with respect to ground, but the matching of the outer coil resistances has been shown conclusively to play a major role.

Quench containment was a very straightforward problem to solve once it was understood. As shown in Section 4.2, this was clearly not a buss or thermal propagation problem. The

cause of the observed quench propagation was due to the L/R time constant of the down ramp changing by a factor of at least a third during the quench of a quarter cell, combined with the high ramp rate sensitivity of certain magnets used in the string tests. As noted, there were also a few quenches that resulted in an apparent containment failure, but were actually due to the way in which the QPS software calculated the dI/dt failure condition which was detected as resistive voltage. Of course, the most conservative response to such a problem with the QPS logic is to activate the strip heaters to quench all the magnets in the protection unit in which there is an inconsistency. This was the response of the QPS. The strand to strand coupling in the cables which leads to these down ramp sensitivities (and the time structure of the field harmonics)[39] as well as higher ramp rate losses has clear implications on accelerator operations and must be minimized. However, the greater the number of magnets being dumped through a given circuit, the smaller the effect of the inductance loss of the given element or sub-element. Therefore, this particular means of propagating a quench should be much less or not at all present in a complete machine.

The question of magnet margin was not answered quantitatively, but the magnets used in this full cell were certainly more than adequate for a 20 TeV machine requiring a $6.5T$ to $6.6T$ peak magnetic field in the dipoles. The actual high field limit of the string was not determined, but the high field limit of an individual dipole had been measured to be in the region of 7300 A during single magnet tests.[15] A full cell power test at 7300 A would have served as an excellent check, but the fact that the string operated reliably within 265 A of the anticipated peak is evidence of the conservative margin inherent in the dipole design.

The strip heater design variation by Haddock *et al.*, clearly shows the importance of balancing the electrical parameters of the heater firing circuit with the down ramp requirements of the system design.[18] The heater circuit RC time constant should be on the order of 10 ms or less to match the order of the thermal diffusion time through the kapton electrical insulation of the strip heater. The resistance of the heater needs to be on the order of 1–10 ohms in order to not require large diameter input cables. The present heaters are fabricated from 25 micron thick stainless steel, but from data obtained from prototype heaters used in model magnet studies, a strip thickness of 12 microns would offer greater flexibility due to a high surface to volume ratio.[29] Recent results from heater studies also indicate that by using better bonding agents, the kapton insulation between heater and coil could be reduced to as little as 75 microns thickness and still allow a five kilovolt hipot between heater and ground (coil plane).[40]

The test involving the upper buss as a protection unit had several unique problems and conditions that could have affected the results (see the detailed discussion at the end of Section 4.6). It should first be noted that the connection between the quad bypass diode lead and the bypass was left in place during the test. It should also be noted that the QPS actually consisted of two distinct but synchronized quench protection monitors, QPM1 and QPM2, and that magnets D4, D5, and Q1 were protected by QPM1 while D6, D7, and D8 were protected by QPM2. This division of logical control could potentially result in up to a 16 ms time difference (one line cycle at 60 Hz) in heater firing commands to the protection strip heaters. This is a small but not negligible effect, and should be accounted for when evaluating heater effectiveness. The magnet used to initiate the quench sequence was D6, but D4 and D5 protected by QPM1 developed resistance faster than the QPM2 protected magnets D7 and D8; thus, it would seem that any delay between QPM1 and QPM2 did not

play a role in the subsequent quenches. This points to the possible effect of the recooler in providing a lower temperature on the downstream side of the half cell protection unit due to the presence of a leaky valve.

The quench generated pressure waves were essentially the same as observed in the half cell tests but possibly slightly reduced. The probable causes of the reduction are the faster quench valve response that resulted from placing pneumatic reserve tanks at the quench valve locations, and the improved quench valve sequencing achieved during the half cell tests. The one additional experiment that was needed, but not attempted due to time constraints, was the activation of only one quench valve (SPR, feed, or end spool) for any quench origin in the full cell. As tested, the maximum pressure that the system would have experienced operationally using the proposed accelerator cryogenic procedures, would have occurred during the magnet cooldown to liquid nitrogen temperatures.

The results of the heat load measurements were not totally satisfactory in that only the magnitudes were obtained, but not the precise locations and causes. The circuit with the greatest uncertainty is the 4 K cold mass circuit whose major load during actual accelerator operations is dynamic due to synchrotron radiation and not static as measured here. The observed heat load magnitude in the 50 mm dipole cryostat would not have been a fatal problem to collider operations, but would have reduced the refrigerator system's reserve capacity, possibly reducing operational performance in the event of a partial refrigerator system failure. However, the heat leaks that appeared to be associated with the spools were much more serious and potentially fatal. Some of the observed load can be attributed to the additional penetrations required to bring out the R&D instrumentation leads utilized in these tests but even these loads should have been minimal provided proper design and construction techniques were followed. Unfortunately, for the spools used in the ASST program, this was not the case, in general. There were various heat shield and penetration problems with the dipole, quadrupole and spool cryostats noted during the assembly periods that needed correction or redesign. In particular, the spool piece penetrations, shield geometries and possibly the supports would have required redesign in order to meet their budgeted loads. The quench valve design needed to be re-examined as the valves had required a great deal of maintenance, repair, and frequent replacement, particularly during the initial operational period. However, the possibility of reducing the required size of the spool penetrations by reducing the size or number of bypass leads, improved valve design and by employing established cryogenic design and manufacturing techniques (which includes tighter quality control during manufacturing) leads to the tentative conclusion that the resulting reduction in heat load, together with a redesign, would have provided spool pieces which would meet the design heat load budget.

REFERENCES

1. T. Dombeck, R. Bork, W. Burgett, J. Gannon, D. Haenni, P. Kraushaar, M. Levin, M. McAshan, A. McInturff, G. Mulholland, D. Murray, R. Nehring, R. Parry, W. Robinson, R. Smellie, F. Spinos, G. Tool and J. Weisend II, "Cryogenic and Power Testing of a String of 50 mm Aperture Dipole Magnets at the Superconducting Super Collider Laboratory", *Int. J. Mod. Phys. A* (proc. Suppl.), **2B** (1993).
2. A. McInturff, S. Augustynowicz, W. Burgett, R. Coombes, C. Dickey, T. Dombeck, W. Fietz, R. Flora, J. Gannon, D. Haenni, P. Kraushaar, M. Levin, M. McAshan, G. Mulholland, D. Murray, W. Robinson,

T. Savord, F. Spinos, G. Tool, J. Weisend II, D. Wallis, D. Voy and J. Zbasnik, "Half Cell Operational Tests of the SSCL", *IEEE Trans. on Applied Superconductivity*, Vol. 3, #1, pp. 740–743, March 1993.

3. W. Burgett, M. Christianson, R. Coombes, T. Dombeck, J. Gannon, D. Haenni, P. Kraushaar, M. Levin, M. McAshan, A. McInturff, G. Mulholland, D. Murray, W. Robinson, T. Savord, R. Smellie, F. Spinos, G. Tool, J. Weisend II and J. Zatopek, "Full Power Test of a String of Magnets Comprising a Half Cell of the Superconducting Super Collider", *Particle Accelerators*, **43**, pp. 41–75, 1993. SSCL-Preprint-162, Oct. 1992, 50pp.
4. P. Kraushaar, "The Accelerator Systems String Test Program", *IISSC Supercollider 5*, edit. P. Hale, pp. 67–70. Plenum Press, New York, 1994. SSCL preprint# 333.
5. A. McInturff, W. Burgett, T. Dombeck, J. Gannon, P. Kraushaar, G. Mulholland, T. Savord, G. Tool, W. Robinson and J. Weisend II, "Test Results and Operational Characteristics of Prototype SSCL Half Cell", Proceeding of the Thirteenth International Conference on Magnet Technology, Victoria, B.C., Canada, September 1993, to be published.
6. J. Weisend II, M. Levin, D. Franks, R. Pletzer, S. Augustynowicz, A. McInturff and W. Boroski, "Heat Leak Performance of the SSC Collider Dipole Magnets", Proceeding of the Thirteenth International Conference on Magnet Technology, Victoria, B.C., Canada, September 1993, to be published.
7. P. Kraushaar, W. Burgett, L. Cromer, J. Gannon, D. Haenni, M. Hentges, T. Jaffery, M. Levin, A. McInturff, G. Mulholland, D. Revell, D. Richter, W. Robinson, D. Voy, J. WeisendII and J. Zatopek, "The SSC Full Cell Prototype String Test", SSCL Preprint 571, November, 1994, Proceedings of '94 ASC, Boston, Oct 1994, to be published.
8. W. Burgett, D. Franks, P. Kraushaar, M. Levin, M. McAshan, A. McInturff, R. Pletzer, D. Revell, W. Robinson, V. Saladin, G. Shuy, R. Smellie and J. Weisend II, "Cryogenic Characteristics of the SSC Accelerator Systems String Test (ASST)", *IISSC Supercollider 5*, edit. P. Hale, pp. 555–558. Plenum Press, New York, 1994. SSCL preprint # 251.
9. L. Coull, D. Hagedorn, V. Remondino, F. Rodriguez-Mateo's, "LHC Magnet Quench Protection System", Proceedings of the Thirteenth International Conference on Magnet Technology, Victoria, B.C., Canada, September 1993, to be published.
10. D. Hagedorn, L. Coull, "Cascade and Multiple Quenching in the Half Octant of the LHC", CERN Internal Note: AT-MA/DH/LC/fl, Note 94–93, February, 1994.
11. D. Hagedorn and F. Rodriguez-Mateos, "Modeling of the Quenching Process in Complex Superconducting Magnet Systems", *IEEE Trans. on Magnetics*, **28**, #1, Jan. 1992, pp. 366–369.
12. A. Devred, private communication.
13. M. Garbor, "Summary BNL Cable Data for SSCL Cable".
14. J. Strait, D. Orris, P. Mazur, M. Bleadon, R. Bossert, J. Carson, S. Delchamps, A. Devred, J. DiMarco, S. Gourlay, R. Hanft, W. Koska, M. Kuchnir, J. Kuzminski, M. Lamm, W. Nah, T. Ogitsu, J. Ozelis, M. Puglisi, J. Tompkins, M. Wake, Y. Yu, Y. Zhao and H. Zheng, "Quench Performance of Fermilab/General Dynamics Built Full Length SSC Collider Dipole Magnets", *IISSC Supercollider 4*, edit. J. Nonte, pp. 365–372, Plenum Press, New York, 1992.
15. A. Devred, T. Bush, R. Coombes, J. DiMarco, C. Goodzeit, J. Kuzminski, W. Nah, T. Ogitsu, M. Puglisi, P. Radusewicz, P. Sanger, R. Schermer, R. Stiening, G. Spigo, J. Tompkins, J. Turner, Y. Yu, Y. Zhao, H. Zheng, M. Anerella, J. Cottingham, G. Ganetis, M. Garber, A. Ghosh, A. Greene, R. Gupta, A. Jain, S. Kahn, E. Kelly, G. Morgan, J. Muratore, A. Prodell, M. Rehak, E. Rohrer, W. Sampson, R. Shutt, R. Thomas, P. Thompson, P. Wanderer, E. Willen, M. Bleadon, R. Bossert, J. Carson, S. Delchamps, S. Gourlay, R. Hanft, W. Koska, M. Kuchnir, M. Lamm, P. Mantsch, P. Mazer, D. Orris, J. Ozelis, T. Peterson, J. Strait, M. Wake, J. Royet, R. Scanlan and C. Taylor, "Review of SSC Dipole Magnet Mechanics and Quench Performance", *IISSC Supercollider 4*, edit. J. Nonte, pp. 113–135, Plenum Press, New York, 1992.
16. J. Tompkins, "Summaries of Iquench vrs Ramp Rate Studies on Full Length 50mm Dipole Magnets", SSCL MD TA241, 1993.
17. A. Lietzke, private communication.

18. C. Haddock, J. Kuzminski, D. Orris and P. Mazer, "Reducing the Energy Requirements of Quench Protection Heaters for the SSC Dipoles – Test Results", *IISSC Supercollider 5*, edit. P. Hale, pp. 611–614. Plenum Press, New York, 1994. SSCL preprint# 318.

19. A. Devred and T. Ogitsu for SSC Magnet R&D Collaboration, "Ramp-rate Sensitivity of SSC Dipole magnet Prototypes", submitted to PAJ.

20. W. Robinson, W. Burgett, T. Dombeck, J. Gannon, P. Kraushaar, A. McInturff, T. Savord and G. Tool, "Electrical Performance Characteristics of the SSC ASST", Proc. 1993 Particle Accel. Conf.", vol. 4, pp. 2731–2735, IEEE Pub. Cat. No. 93CH3279-7, (1993).

21. P.S. Martin, "Design and Operation of the Quench Protection System for the Fermilab Tevatron", AIP Conference Proceedings 184, Physics of Particle Accelerators, Vol. 2, 1989, pp. 2073–2098.

22. J. Strait, "DCA312 Quench Current versus Temperature", FNAL Report, TS-SSC 91-250, Dec 18, 1991.

23. J. P. Ozelis, S. Delchamps, S. Gourlay, T. Jaffery, W. Kinney, W. Koska, M. Kuchnir, M. Lamm, P. Mazer, D. Orris, J. Strait, M. Wake, J. Dimarco, J. Kuzminski and H. Zheng, "AC Loss Measurements of Model and Full Size 50mm SSC Collider Dipole Magnet at Fermilab", IEEE Trans. Applied Superconductivity, vol. 3, #1, pp. 678–681 (1993).

24. J. Tompkins, "AC Losses for ASST Dipoles", SSCL MSD-TA-247.

25. S. Delchamps, R. Hanft, T. Jaffery, W. Kinney, W. Koska, M. Lamm, P. Mazer, D. Orris, J. Ozelis, J. Strait and M. Wake, "AC Loss Measurements of SSC Dipole Magnets", Proced. ICFA Workshop on AC Superconductivity" ACSC92, National Lab for HEP, Tsukula, KEK Proceedings 92–14, pp. 19–22 (1992).

26. S. Johnson, "Parameters Affecting Temperature in Magnet Coil", SSCL Magnet Division Test & Analysis Note, MD-TA-230, 925830 RM, Aug 12, 1992.

27. S. Johnson, "Maximum Temperature in DCA321 Magnet Coil during Spot heater Induced Quenches", SSCL MDTA-229, 1992.

28. A. McInturff, J. Weisend II, C. Dickey, R. Flora and D. Wallis, "Measured Control Characteristics of the Half Cell 40mm Aperture Magnet String", *IISupercollider 4*, edit. J. Nonte, pp. 859–866, Plenum Press, New York, 1992.

29. A. McInturff, R. Flora, B. Norris, J. Theilacker, D. Wolf, S. Augustynowicz, C. Dickey, G. Tool, D. Wallis and J. Weisend II, "Half Cell 'SSC' 40mm Aperture Magnet String", IEEE Trans. on Magnetics, Vol 28, #1, p. 512, Jan. 1992.

30. C. Haddock, "Quench Protection Heater Data Bibliography", SSCL Internal Note MD-MJG-0-93-017.

31. C. Haddock, R. Jayakumar, F. Meyer, G. Tool, J. Kuzminski, J. DiMarco, M. Lamm, T. Jaffery, D. Orris, P. Mazur, R. Bossert and J. Strait, "SSC Dipole Protection Heater Development", IEEE Trans. on Magnetics, Vol 28, #1, post publication, Jan. 1992.

32. C. Haddock, B. Aksel, F. Meyer, J. Jayakumar and G. Tool, "SSC Dipole Quench Protection Heater Test Results" Proc. 1991 Particle Accel. Conf.", vol. 4, pp. 2215–2217, IEEE Pub. Cat. No. 91CH3038-7, (1991).

33. J. Strait, B.C. Brown, J. Carson, N. Engler, H.E. Fisk, R. Hanft, K. Koepke, E. Larson, R. Lundy, P. Mantsch, P.O. Mazur, A.D. McInturff, T. Nicol, T. Ohmori, E.E. Schmidt, J. Theilacker and G. Tool, Fermi National Accelerator Laboratory: J. Cottingham, P. Dahl, M. Garber, A. Ghosh, C. Goodzeit, A. Greene, J. Herrera, S. Kahn, E. Kelly, G. Morgan, A. Prodell, W. Sampson, W. Schneider, R. Shutt, P. Thompson, P. Wanderer and E. Willen, Brookhaven National Laboratory: and S. Caspi, W. Gilbert, W. Hassenzahl, R. Meuser, C. Peters, J. Rechen, R. Rover, R. Scanlan and C. Taylor, Lawrence Berkeley Laboratory, "Full Length Prototype SSC Dipole Test Results", *IEEE Trans. Magnetics*, MAG-23, No. 2, pp. 1208–1214, March 1987.

34. G. Tool, R. Flora, P. Martin, D. Wolff, "Energy Saver Partial Ring Power Tests", IEEE Transactions on Nuclear Science, NS-30, # 4, August, 1983, pp. 2889–2891.

35. R. Flora, J. Saarivirta, G. Tool and D. Voy, "The Energy Saver/Doubler Quench Protection Monitor System", IEEE Transactions on Nuclear Science, NS-28, #3, pp. 3289–3291, June, 1981.

36. J.R. Sanford and D.M. Matthews, Eds., "Site Specific Conceptual Design of the Super Conducting Super Collider", SSCL-SR1056 (1990).

37. B. Daniels, R. Parry, B. Hendrix, V. Oliphant and C. Hamm, "ASST Safety Analysis Report (SAR)", SSC Laboratory, DMP-000001, January, 1992.

38. R. Carcagno, M. McAshan and W. Schiesser, "Helium Venting Model for a SSC Half Cell", *IISSC Supercollider III*, edit. J. Nonte, pp. 833–847, Plenum Press, New York, 1991.

39. T. Ogitsu, Y. Zhao, A. Akheiov and A. Devred," Influence of Cable Eddy Currents on Magnetic Field Harmonics", Proced. ICFA Workshop on AC Superconductivity" ACSC92, National Lab for HEP, Tsukula, KEK Proceedings 92–14, pp. 23–27 (1992).

40. A. McInturff, private communication.